THESIS/
REPORTS
ALBINI,
F.A.

Fire behavior induced by helicopter rotor wash

Frank A. Albini

COOP AGREE MONT STATE UI

FINAL REPORT FOR COOPERATIVE AGREEMENT
#INT-97071-COA
"Helicopter Induced Fire Behavior"
MONTANA STATE UNIVERSITY
FS Contact: Dr. Gregg M Johnson
CoOp Contact: Dr. Frank Albini

Fire behavior induced by helicopter rotor wash

Frank A. Albini
Research Professor
Mechanical and Industrial Engineering
Montana State University
Bozeman MT 59717-3800

(406) 994 - 6298
FAX (406) 994 - 6292
e-mail: falbini@me.montana.edu

ABSTRACT

Simplified analytical models for downwash flows from helicopters and for their interactions with a flat surface covered by vegetation permit evaluation of peak local horizontal wind speed and the consequent increase in surface fire spread rate and flame length. A similarly simple model for the outwash flow field permits estimation of the maximum transport distance of a potential firebrand. Interaction between the downwash flow and the relative wind due to the combined effects of helicopter velocity and ambient wind includes only an increase in an air entrainment parameter and estimation of a maximum altitude for model validity based on predicted deflection of the downwash flow to 30 degrees from vertical. The models are incorporated into interactive programs for personal computers.

INTRODUCTION

Use of helicopters in wildland fire suppression operations has increased steadily for the last few decades. The roles they now routinely undertake include deployment of helitack crews, transport of critical supplies and key overhead personnel, intelligence, monitoring of operations, and delivery of water or fire retardant in direct tactical suppression actions. In such actions it is often necessary for the delivery helicopter to fly over or even to hover over the fire edge. When this is done, downwash from the helicopter can interact with the fire, causing a temporary local increase in spread rate and flame length. Occasionally rotor wash can scatter firebrands that start spot fires right where an effective suppression treatment has just been applied, negating an expensive and hazardous operation. To minimize such unfortunate occurrences, the National Wildfire Suppression Technology (NWST) group of the USDA Forest Service is developing decision aids to support fire-related helicopter operations.

USDA Forest Service has developed a data base of near-surface wind speed measurements taken during helicopter overflights of anemometer arrays [Teske and Kaufman 1994, Teske *et al* 1995] for use in this endeavor and in regard to helicopter delivery of aerial pesticide sprays. In addition to these basic data measurement programs, NWST sponsored research at Montana State University, Bozeman, through a Cooperative Research and Development Agreement, to build simulation models to facilitate prediction of the fire behavior implications of helicopter rotor wash. This paper outlines the models developed in this effort and presents some results derived from them. Models are presented for the downwash and the outwash (outward flow over the surface) flow fields, providing a map of the air velocity everywhere beneath the helicopter. In addition, flight of a firebrand particle transported by the outwash flow is modeled and an algorithm developed for predicting maximum potential spotting distance.

HELICOPTER - INDUCED AIR FLOWS

Helicopters are sometimes called "rotary wing aircraft" because it is the lift generated by their airfoil-shaped rotors that allow them to fly. Air flow through the plane of a spinning rotor is accelerated downward in the same way that air flowing past a conventional aircraft wing is accelerated downward, creating a difference in static pressure between the upper and lower wing surfaces. This pressure difference, multiplied by the area of the wing, is the lift force, and it can be calculated in this way.

But lift can also be calculated by examining the effects of the equal and opposite force acting on the air stream. The effect of this force is to create a net flux of momentum downward. That is, if the vertical component of the vector velocity of the air is examined at each point in a horizontal plane situated far enough below an aircraft that the static pressure is essentially constant at its hydrostatic equilibrium value, and in another plane similarly situated above the aircraft, it will be found that there is an excess flux of momentum downward through the lower surface beyond that through the upper surface. This net momentum flux is equal and opposite to the lift force, by Newton's second law.

Using the momentum flux principle just described, and treating the downwash air flow as a circular jet of incompressible fluid, one can relate the downward velocity of the flow just below the helicopter to the gross weight of the helicopter (*i.e.*, the lift needed to sustain it) and the area swept out by the rotor(s). This relationship is derived in appendix A and graphed in figure 1. This figure shows the characteristic (peak) velocity predicted to occur in the downwash flow, at a point just below the helicopter, as a function of the ratio of the gross weight of the helicopter to the total rotor plane area, called the "rotor plane loading". Values of this parameter for several helicopter types that sometime see fireline duty are given on figure 1.

Also presented in appendix A is the mathematical model for the entrainment of air into the downwash flow. The entrainment process increases the downward mass flow of air with distance from the helicopter. But because the downward momentum flux (the product of mass flow and velocity) is nominally constant, the flow velocity decreases and the cross sectional area (or the radius) of the flow increases with distance from the helicopter. So the growth of the downwash radius and the decay of the downwash velocity depend directly upon the rate of air entrainment.

The entrainment process for fully developed, turbulent jet-like flow through a still ambient environment is well modeled by equating the inward radial flow velocity to a fraction of the axial velocity. The fraction is called the "entrainment parameter" and its value for circular jets has been empirically established as about 0.08 [Ricou and Spalding 1961]. But when there is a relative velocity between the ambient air and the axis of the jet, the situation is not so easily modeled. For the purpose of the present work, an upper limit is sought to the influence of the helicopter-induced flow on fire behavior. So an upper limit is sought for the velocity of the downwash flow as it interacts with the surface. For this purpose, the relative velocity (the difference between the ground velocity of the helicopter and the local wind velocity) is essentially ignored until it reaches a magnitude comparable to the maximum axial velocity of the downwash flow. When this situation obtains, the model for the process shifts from still air entrainment to the incorporation of impinging flow on the upwind side, with the result that an effective entrainment parameter is defined. This parameter varies with the ratio of the crossflow velocity to the characteristic (maximum) downwash velocity in the arbitrary smooth manner shown in figure 2.

The downwash flow is treated as being vertical so long as its lateral deflection by the relative wind allows its axis to remain within 30 degrees of vertical. As lateral momentum is accrued by the downwash flow,

(what wind speed caused axis to be greater than 30°

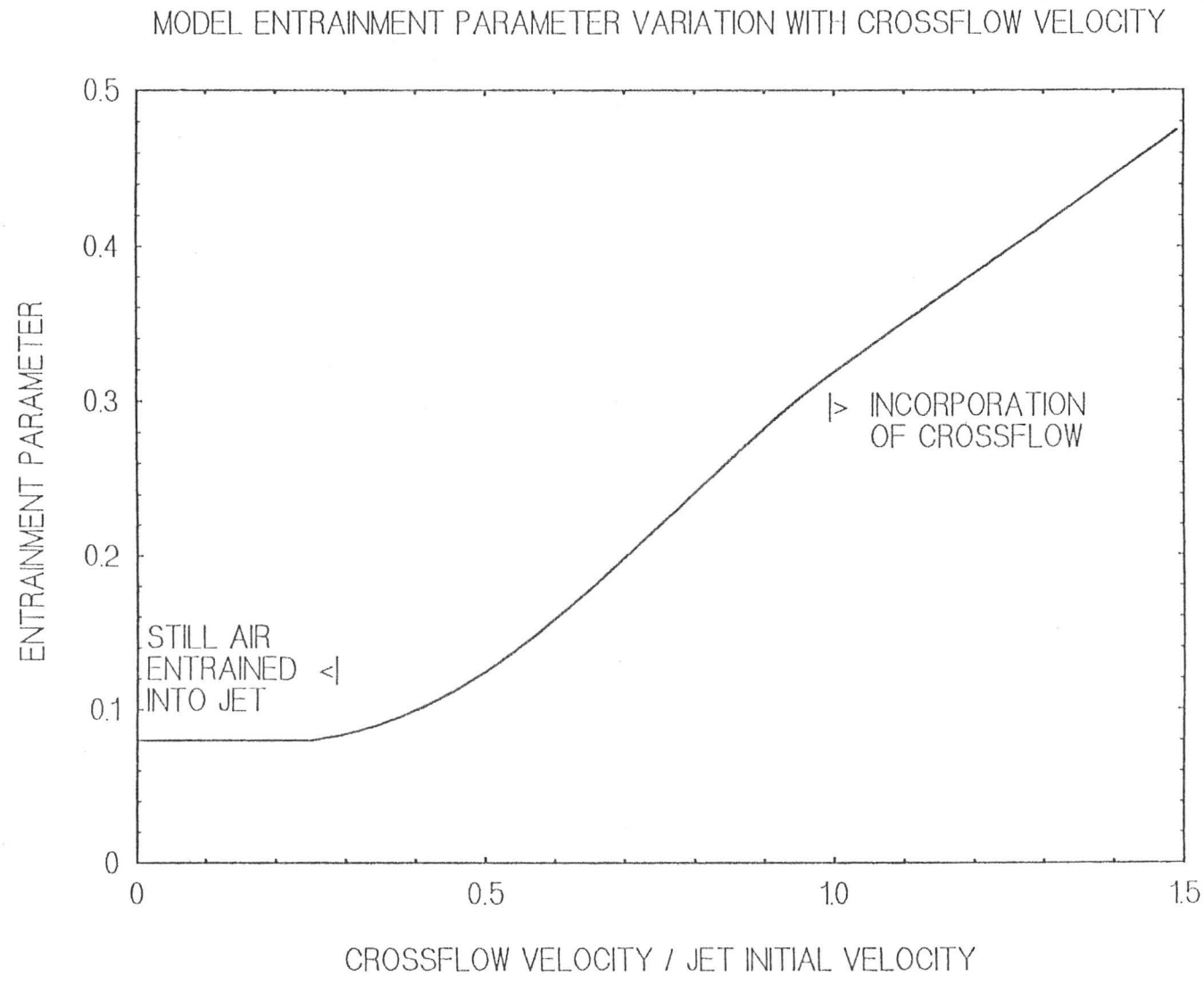

Figure 2. Entrainment parameter variation with relative air speed used in downwash flow model.

the axis of the downwash stream bends in the direction of the crosswind. When the axis direction predicted by the model reaches 30 degrees from vertical, the model is thought to be no longer trustworthy, and it should not be used. The altitude and relative wind speed combinations that lead to this demise of the model are illustrated in figure 3. This figure plots helicopter altitude, normalized by rotor radius, versus relative air speed normalized by characteristic downwash velocity (from figure 1). The curve divides this plane into two regions. To the right, the cross wind deflection of the downwash jet should cause it to impinge the surface at an angle of 30 degrees or more from the vertical. To the left, this angle would be 30 degrees or less, and the models subsequently described are presumed to be adequately reliable in the "upper bound" sense described above. The arbitrary nature of this criterion is apparent. The equations given in appendix A for the deflection from vertical of the downwash axis can be used to establish other rules for when to use and when not to trust the flow structure models.

When the vertical flow impinges on the surface, it turns abruptly and flows radially outward from the centerline of the downwash flow. In making the abrupt change of direction, the turbulence intensity increases locally and there is a net loss of kinetic energy to heat generation. By analogy with the turbulent flow of fluid through pipe "tee" fittings, which have been the subject of many engineering measurements, it appears that the 90 degree turn should cost the fluid at least half its kinetic energy. Since the "worst case" is sought here, this is the loss factor used in the model for turning the vertical flow to horizontal. A model for the horizontal (or "outwash") flow field is presented in appendix B, including the boundary conditions that link the radial and vertical flow fields.

The outwash flow field is modeled as entraining air from the still ambient along its upper surface and experiencing resistive shear stress at its lower surface due to interaction with a vegetation cover layer.

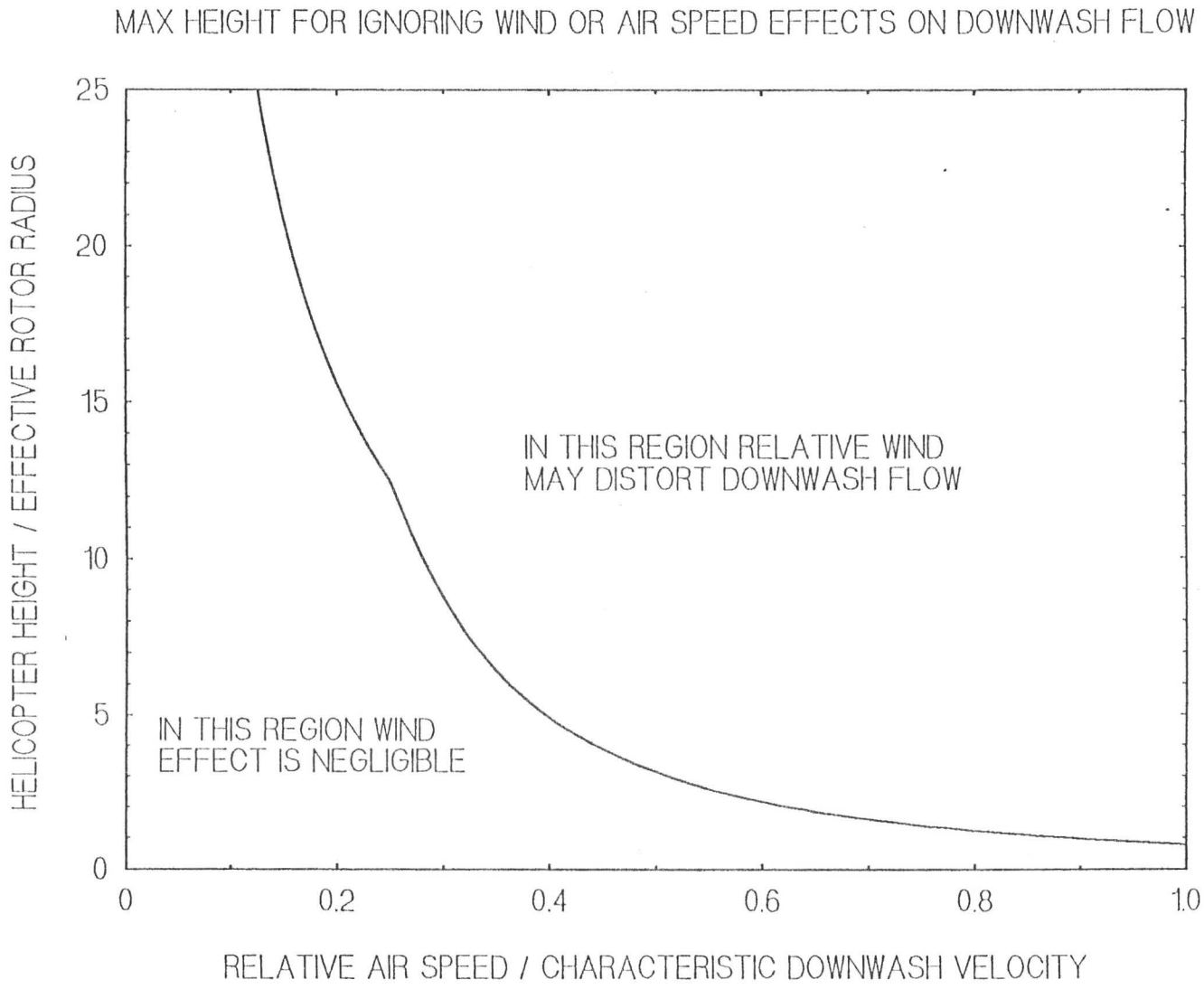

Figure 3. Relationship between helicopter height and air speed for which the effect of cross wind on the downwash flow model is thought to be significant.

Since the geometry of the outwash flow more closely mimics that of a two dimensional line plume than a circular jet, the examples presented in figures 4 and 5 are based on the entrainment parameters empirically found for buoyant line plume sources [Rouse, Yih, and Humphreys 1952; Lee and Emmons 1961].

Figure 4 shows the dividing streamline between still ambient air and the downwash and outwash flows, plotted in terms of distances normalized by helicopter rotor radius. The lower limit to the height of the outwash flow layer as a function of radial position is established by treating the surface as being free of friction. When a vegetation layer is present, a surface skin friction coefficient of 0.32 [Albini 1981a] is imposed, which slows the flow and deepens the outwash layer. This is apparent from figure 5, which graphs the outwash velocity versus radial position. This figure shows the speed reduction becomes a large fraction of the friction-free speed within a rotor radius or two of radial travel.

SPREAD RATE AND FLAME LENGTH IMPLICATIONS

The horizontal air speed in the outwash flow increases the spread rate of any surface fire present. The local wind field and the outwash velocity field cannot simply be summed, so it presumed here that the helicopter-induced flow dominates the local wind field. If not, the helicopter-induced enhancement of fire spread rate is no more important than the effect of wind already present. Figure 6 shows the maximum outwash velocity over a smooth surface versus the altitude of a helicopter hovering in still air, for various rotor radii. The maximum horizontal velocity is shown, which occurs at the point where the downwash and outwash flow fields abut; its magnitude is independent of any vegetation cover layer.

When there is a relative velocity between the downwash flow and the ambient air, the effective entrainment parameter is increased, as described above. This effect is included in the relationships

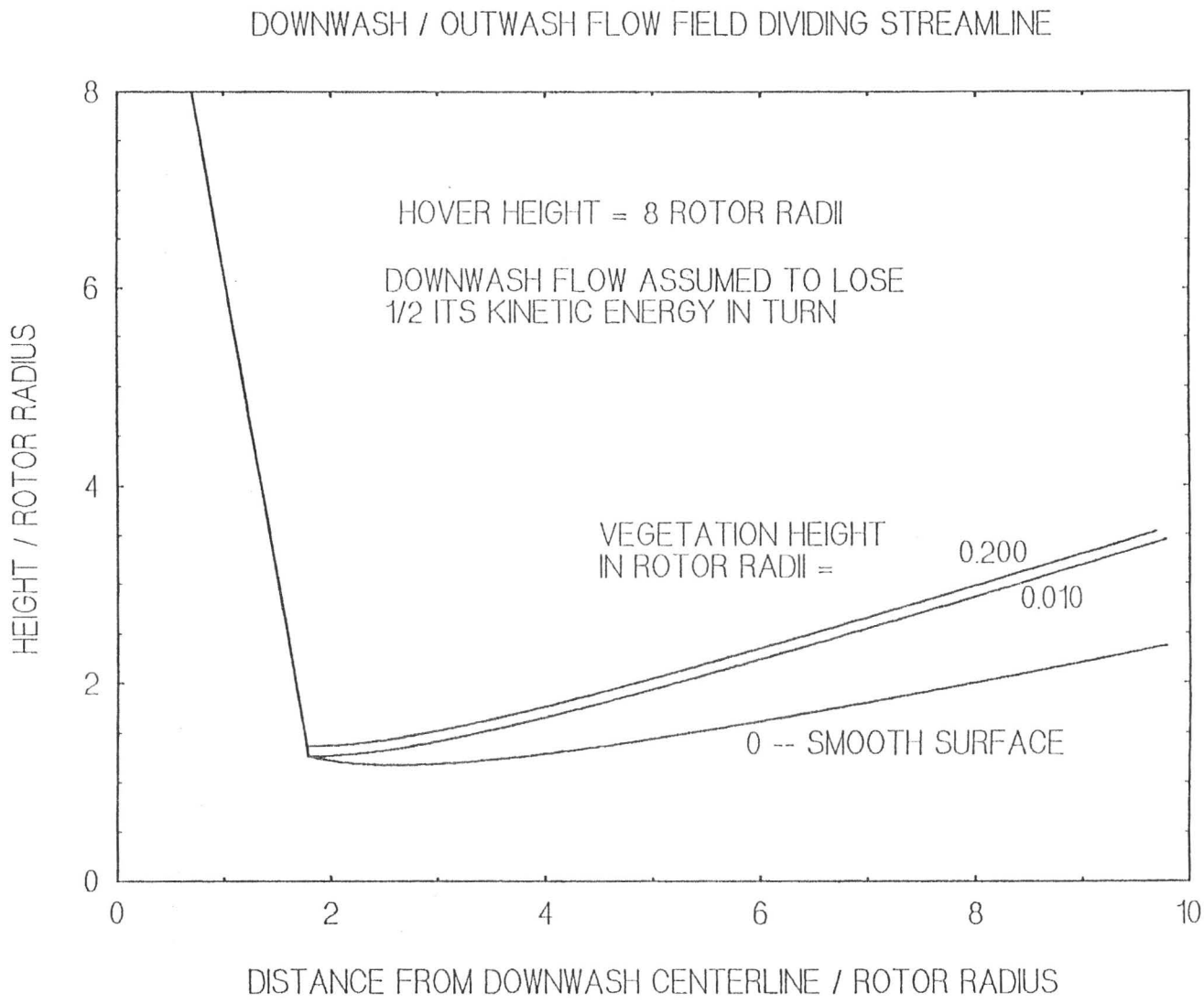

Figure 4. Model predictions of the location of the dividing streamlines of downwash and outwash flows for a helicopter hovering in still air.

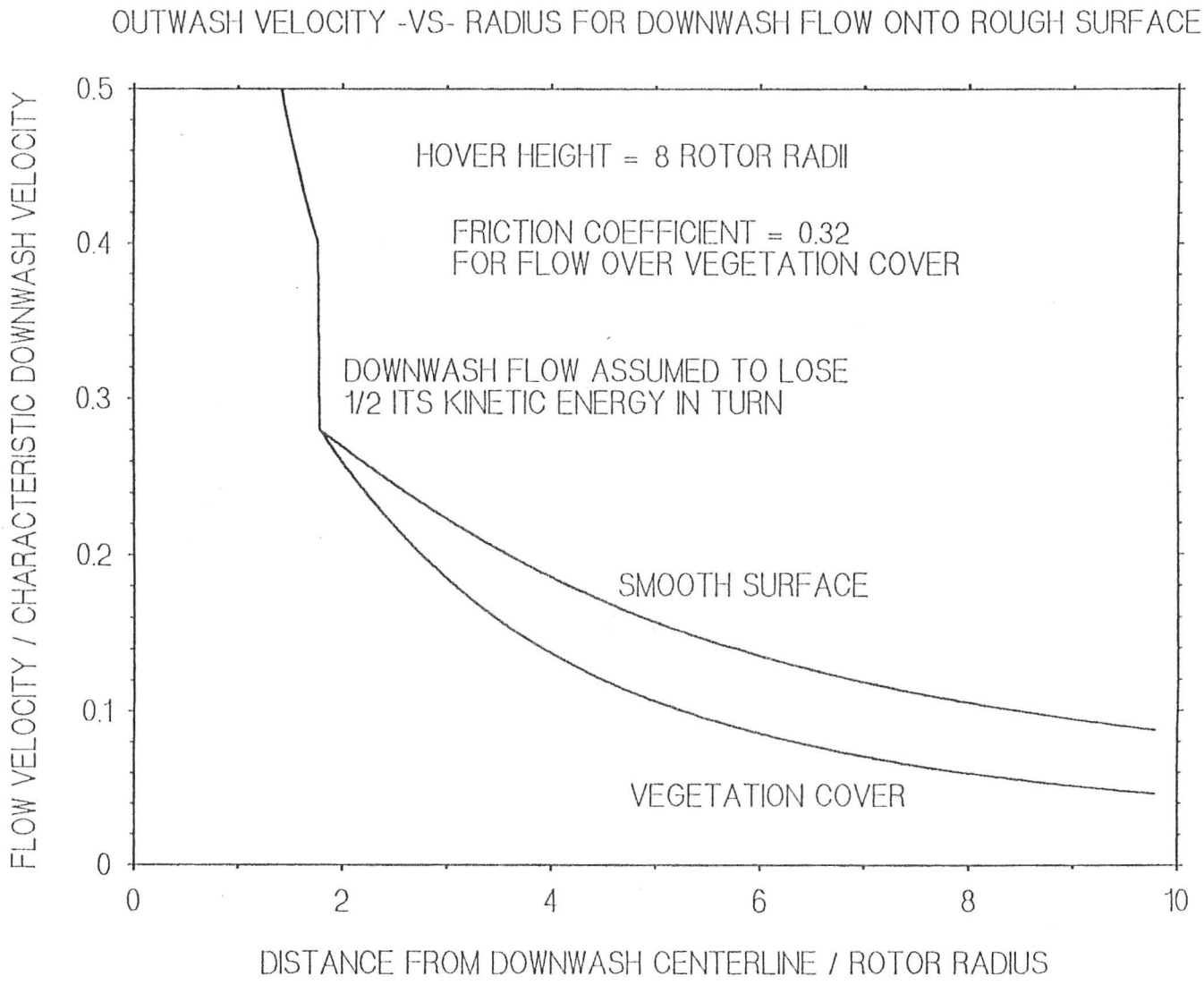

Figure 5. Model predictions of velocity variations in downwash and outwash flows for a helicopter hovering in still air.

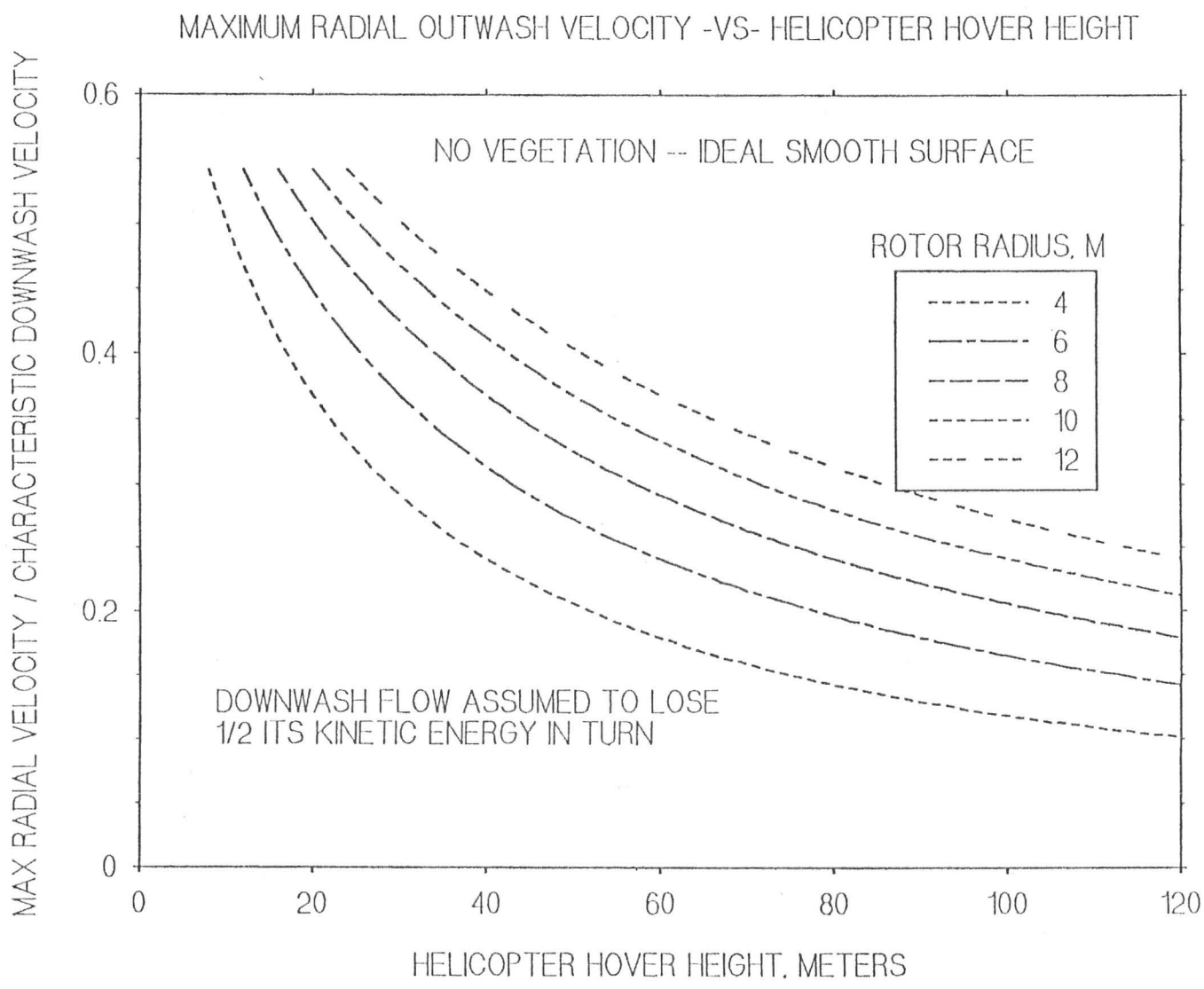

Figure 6. Predicted maximum radial outwash velocity as a function of helicopter hover height in still air, for various rotor radii. The surface is taken to be frictionless and free of vegetation, but these assumptions do not change the predicted maximum radial velocity.

graphed in figures 7 - 9, which show maximum outwash velocity versus helicopter hover height for rotor radii of 4 , 8 , and 12 meters respectively. Another parameter on these graphs is the ratio of the relative lateral velocity to the characteristic downwash velocity. It is apparent that this parameter is almost inconsequential except that it determines where the model becomes suspect. The enhanced entrainment associated with the cross wind does not change the peak outwash velocity significantly. (It does, however, alter the mass flow in the downwash column, and hence the initial depth of the outwash flow layer, and therefore the capacity of the outwash to transport firebrands, as discussed below.)

The figures described above allow graphical determination of maximum outwash velocity as a function of helicopter gross weight, rotor radius, altitude, and air speed (or ground speed and wind velocity), and the equations given in appendices A and B offer a means of calculating it. The influence of this local wind on fire behavior depends upon the nature of the fuel. The BEHAVE fire behavior prediction system [Burgan and Rothermel 1984, Andrews 1986, Andrews and Chase 1989], widely used by wildland fire agencies in the United States and elsewhere, employs the formulation of Rothermel [1972] to predict the effect of wind on fire spread rate and flame length. This formulation provides a multiplying factor for the zero-wind rate of spread that depends upon the wind speed and the fuel type (one of 13 generic descriptions provided by the BEHAVE system) that best fits the fuel being considered. In this system, the flame length is predicted using an empirical formula due to Byram [see, *e.g.* Rothermel 1972]. The wind sensitivity of this predictor reduces to a multiplying factor for the zero-wind flame length that is simply the spread rate multiplying factor raised to the power 0.46. For convenience, the spread rate and flame length multiplying factors are given both graphically and in tabular form in appendix C.

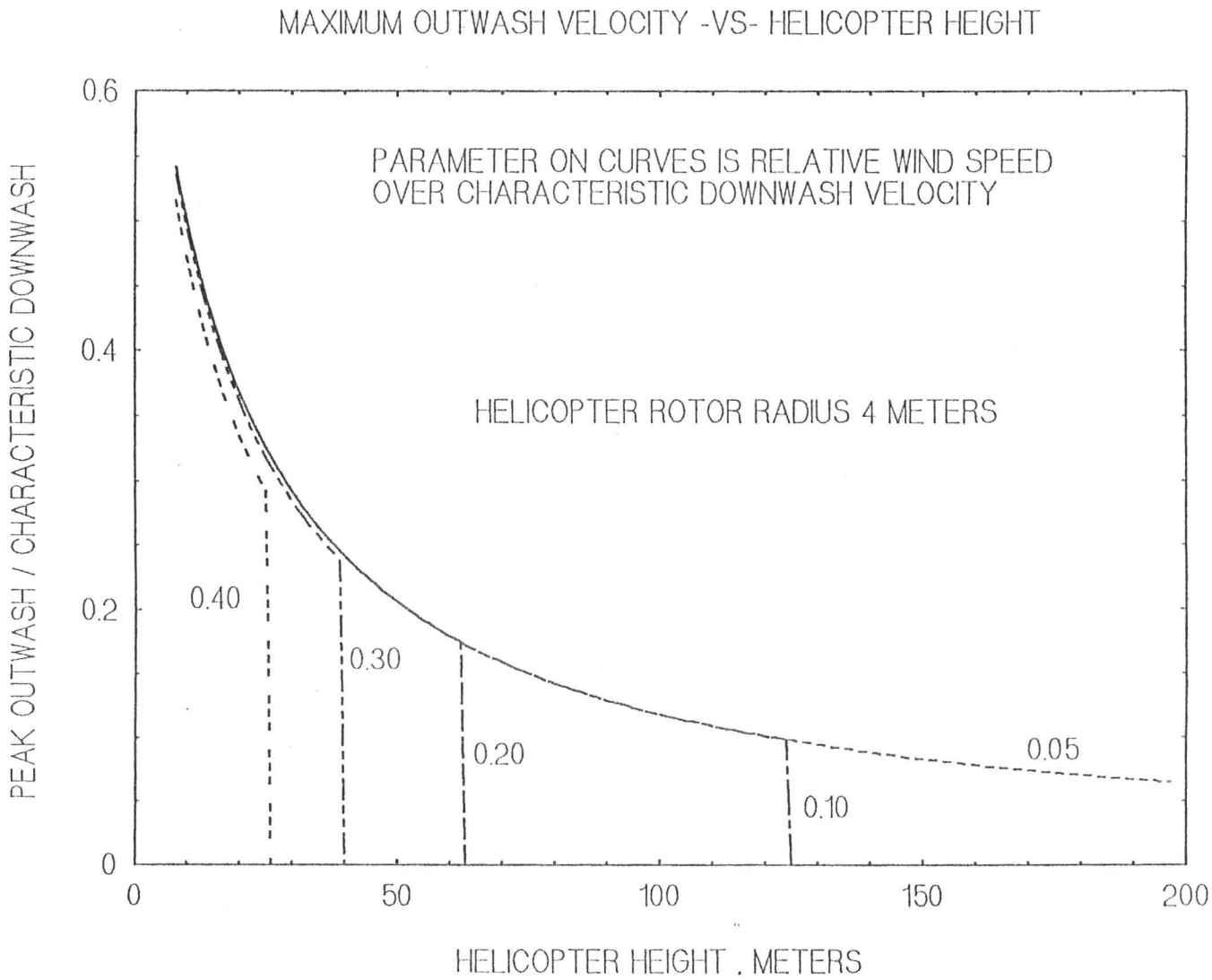

Figure 7. Predicted maximum radial outwash velocity as a function of altitude for a helicopter with a 4 meter rotor radius, at various wind speeds relative to the helicopter. Indicated model collapse conditions correspond to the curve of figure 3.

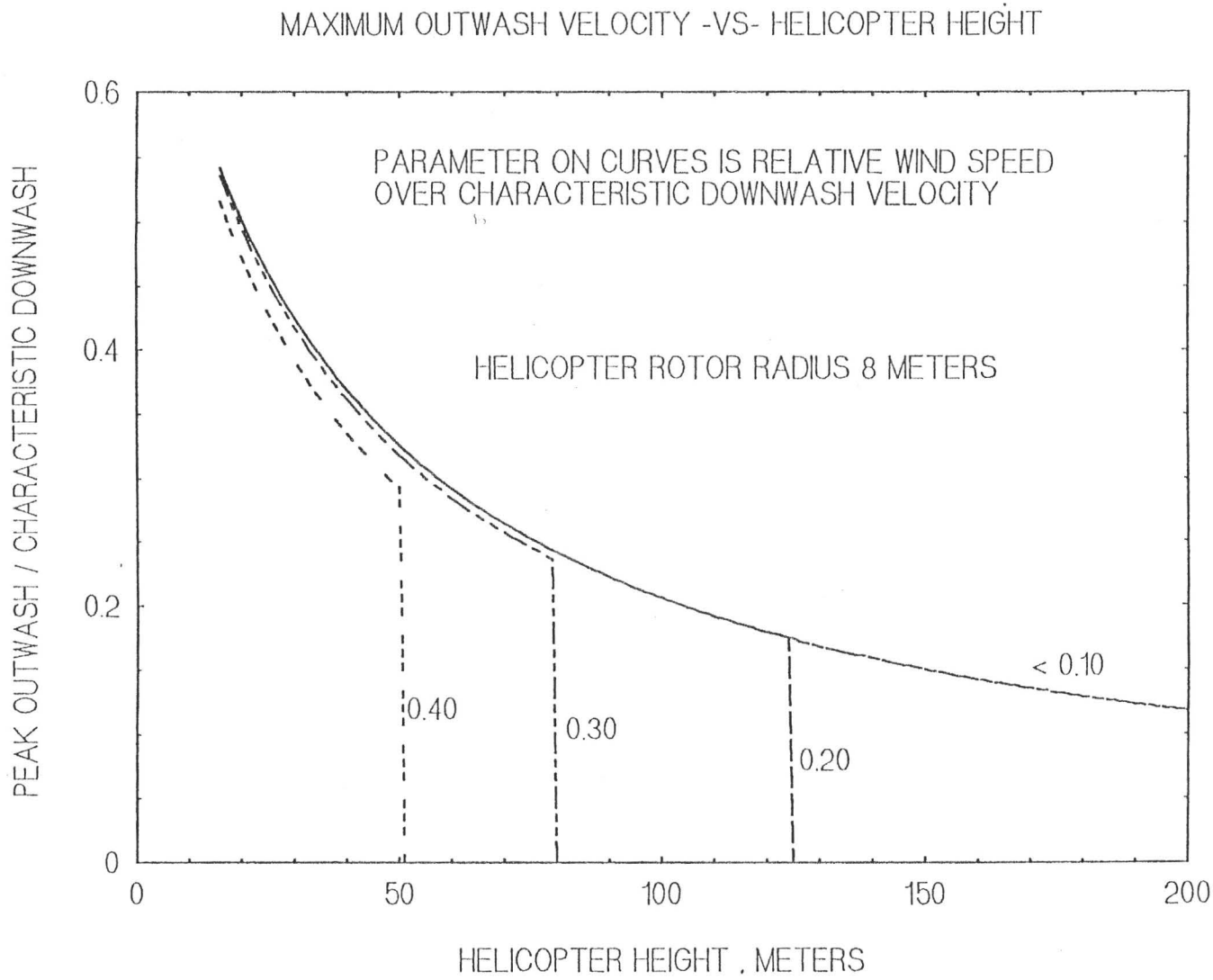

Figure 8. Predicted maximum radial outwash velocity as a function of altitude for a helicopter with a 8 meter rotor radius, at various wind speeds relative to the helicopter. Indicated model collapse conditions correspond to the curve of figure 3.

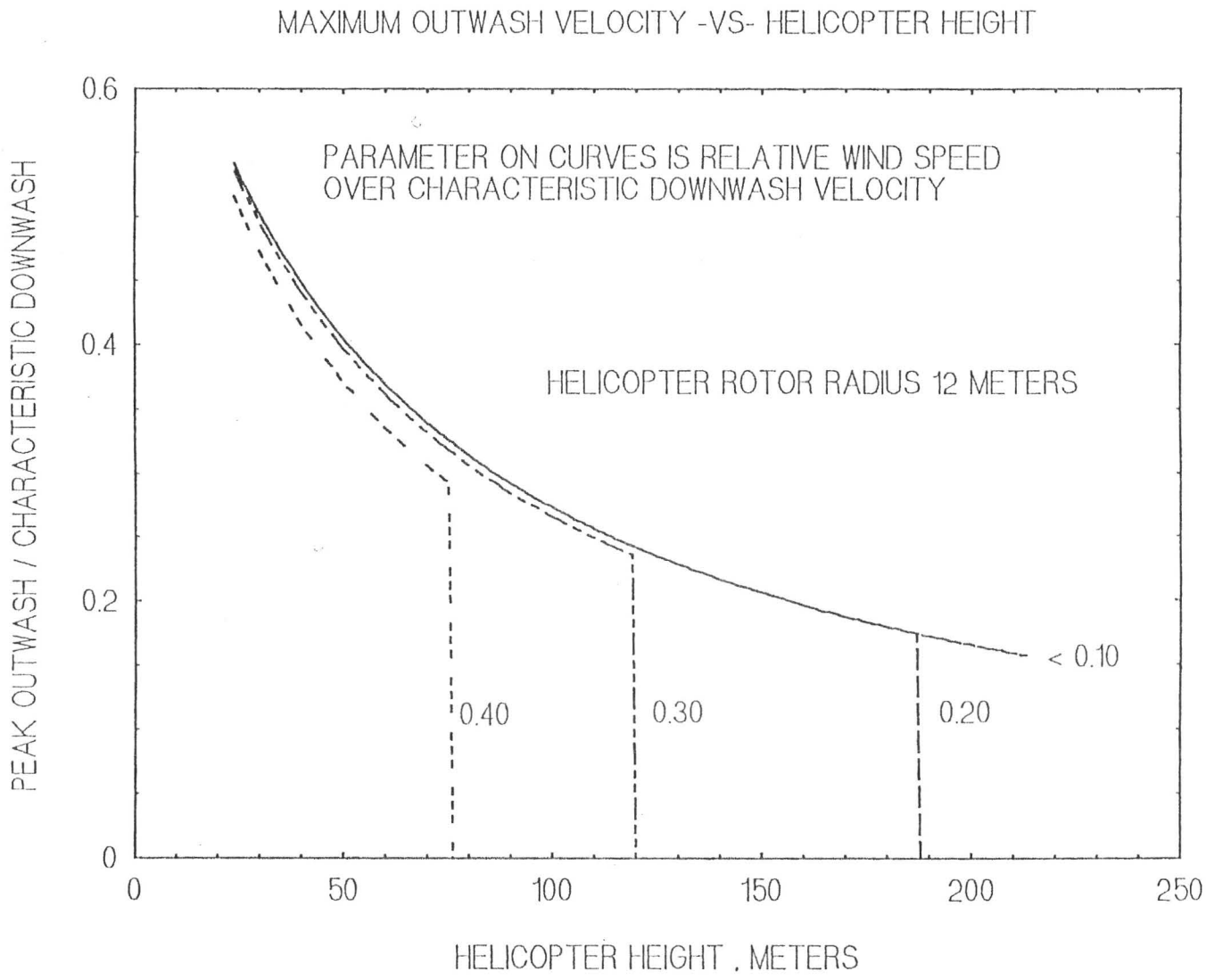

Figure 9. Predicted maximum radial outwash velocity as a function of altitude for a helicopter with a 12 meter rotor radius, at various wind speeds relative to the helicopter. Indicated model collapse conditions correspond to the curve of figure 3.

FIRE SPOTTING IMPLICATIONS

It is important to establish a clear mental picture of the situation as modeled to understand how the potential spotting range calculations are to be interpreted. The helicopter can be imagined to fly over a surface fire at some constant speed and altitude. The downwash column created by the helicopter moves over the ground at the true speed of the helicopter. The place on the ground where the centerline of the downwash impinges will not be directly beneath the helicopter. If there is no wind, the impingement point will trail along behind the helicopter. If one wishes to calculate the location of this point relative to the helicopter, one can determine the path of the downwash centerline by integrating the slope of the centerline (tangent of angle θ in equation A12) as a function of z, distance below the helicopter. But the relative location of the place where the downwash interacts with the surface is not relevant to the capability of the flow field to transport firebrands. For this purpose, one need only model the outwash flow field and its movement over the ground. This is the procedure used here.

General equations for modeling the trajectory of a burning firebrand in a nonuniform wind field were presented by Albini [1979, 1981b] for an empirical firebrand burning rate model. These equations are recapitulated in condensed form for the present application in appendix D. Analysis of potential spotting attributable to the flight of a helicopter over a wildland fire permits some simplification of the general problem, because interest is focused here on the prompt occurrence of spot fires. So firebrand transport distance are relatively short, since they must be physically large enough either to continue flaming during flight or to burst into flame upon alighting. These requirements can be translated loosely into requirements on minimum cylindrical particle diameter and mass density (see appendix D) which, coupled with the flow velocity levels expected, mean that the particles should travel on the order of 10 seconds.

Therefore it is not necessary to model the loss of particle mass, since this will not significantly alter the trajectory; in other words, candidate firebrands can be treated as inert particles with fixed properties.

To determine the maximum distance that a viable firebrand might be transported by the outwash flow, a search is performed over the parameter space that determines the particle trajectories. It is presumed that firebrand particles are scrubbed up from the surface (or taken from the small branches of vegetation somewhere near the surface) in the highly turbulent region where the downwash flow interacts with the surface, turns, and begins to flow radially outward. In this region large scale eddies undoubtedly occur, leading to temporary large air velocities in virtually all possible directions. The ability of this flow field to launch particles is established, in an upper bound sense, by imagining that air flows upward at the velocity with which the downwash flow reaches the surface. The duration of such a hypothetical "vertical gust" should not exceed either the time it would take for a mass of air to travel from the surface to the initial mean height of the outwash flow at this maximum local speed, or the time it would take for the helicopter to travel a distance equal to the minimum radius of the downwash flow (see appendix A). So the minimum of these two times is established and the motion of a candidate firebrand particle is simulated for that period of time.

The candidate particle starts from rest on the surface at some point on a circle of radius 10% greater than the maximum radius of the downwash flow. It is transported upward until the time allotted expires. (The algorithm actually allows for the possibility that the particle reaches the upper surface of the initial outwash flow and is injected into the still ambient air, but this situation never arises using the time limits just described.) The initial height of the candidate particle is thus established, as is the speed at which it is traveling initially. Its starting location is allowed to range over half the circumference of the maximum

downwash flow boundary, and its initial direction of motion is freed to range over elevation angles from horizontal to near vertical, and all azimuth angles that can lead to large transport distances.

The trajectory of the candidate particle is then simulated by numerical integration of its equations of motion (appendix D). As time elapses the flow field which transports the particle moves at the ground speed of the helicopter, so the environment being experienced by the particle evolves in a complicated way. It may initially be moving ahead of the helicopter only to be overtaken and driven earthward by the downwash column later.

The flight of the candidate particle ends when it returns to the height of the top of the vegetation layer. When this occurs, the distance which it has traveled from launch point to impact is calculated along the direction of the helicopter's ground track (the "along-track" range) and perpendicular to this direction (the "cross-track" range). In each direction only the absolute value of the distance is considered. In addition, the distance without regard to direction is also determined. The initial conditions (location and velocity) of the particle's flight are allowed to vary over a wide range, as indicated above, and the maximum spotting ranges determined. Finally, the candidate particle "size" is allowed to vary upward from the minimum value thought to represent a viable firebrand to a maximum of approximately twice the minimum. So long as the predicted maximum spotting range (regardless of direction) continues to increase, the next larger particle size is considered. But as soon as the predicted maximum spotting range declines with an increase in particle size, the parameter sweep is terminated.

An experienced numerical analyst will have noted that the separation between the various flow fields (downwash, outwash, and still ambient) has been described as abrupt in the discourse above. In the

numerical integration of particle trajectories, a "transition layer" between each of the flow fields is simulated, to make the transition from one condition to the other less abrupt. This is done to keep the equations of motion from being what numerical analysts would describe as "stiff" [Press *et al* 1994]. A transition layer around the downwash flow field is modeled as having radial extent equal to 10% of the radius at which the transition to outwash flow occurs. The upper boundary of the outwash flow field is also capped by a transition layer of vertical dimension equal to 10% of the local thickness of the outwash layer. In these transition zones, flow velocity decreases linearly with distance from its value within the modeled zone to zero at the ambient edge. This artifice permits the use of a much bigger time step in the simulation without the pitfall of numerical instability which would otherwise arise almost inevitably.

The firebrand trajectory simulation algorithm is embedded in an interactive computer program that facilitates the specification of conditions to be simulated. Input data required include the gross weight and rotor radius of the helicopter, depth of the surface vegetation layer, ambient wind speed, and wind direction relative to the true velocity of the helicopter. In addition, a range of helicopter heights above ground can be specified, and up to six ground speeds for the helicopter. The program will then create three output files (with user-specified names) one each for maximum potential spotting distances in the along-track and cross-track directions, and one for maximum distance without regard to direction. Examples of the spotting distance predictions of this program are exhibited in figures 10 - 18.

Figures 10 shows the predicted maximum cross-track spotting distance for what will be called nominal conditions. A CH-47 Chinook helicopter of 12,000 kg (near empty) gross weight is flying over vegetation cover of height 200 cm. The range of altitudes is 20 - 140 m and true ground speeds of 0, 2,

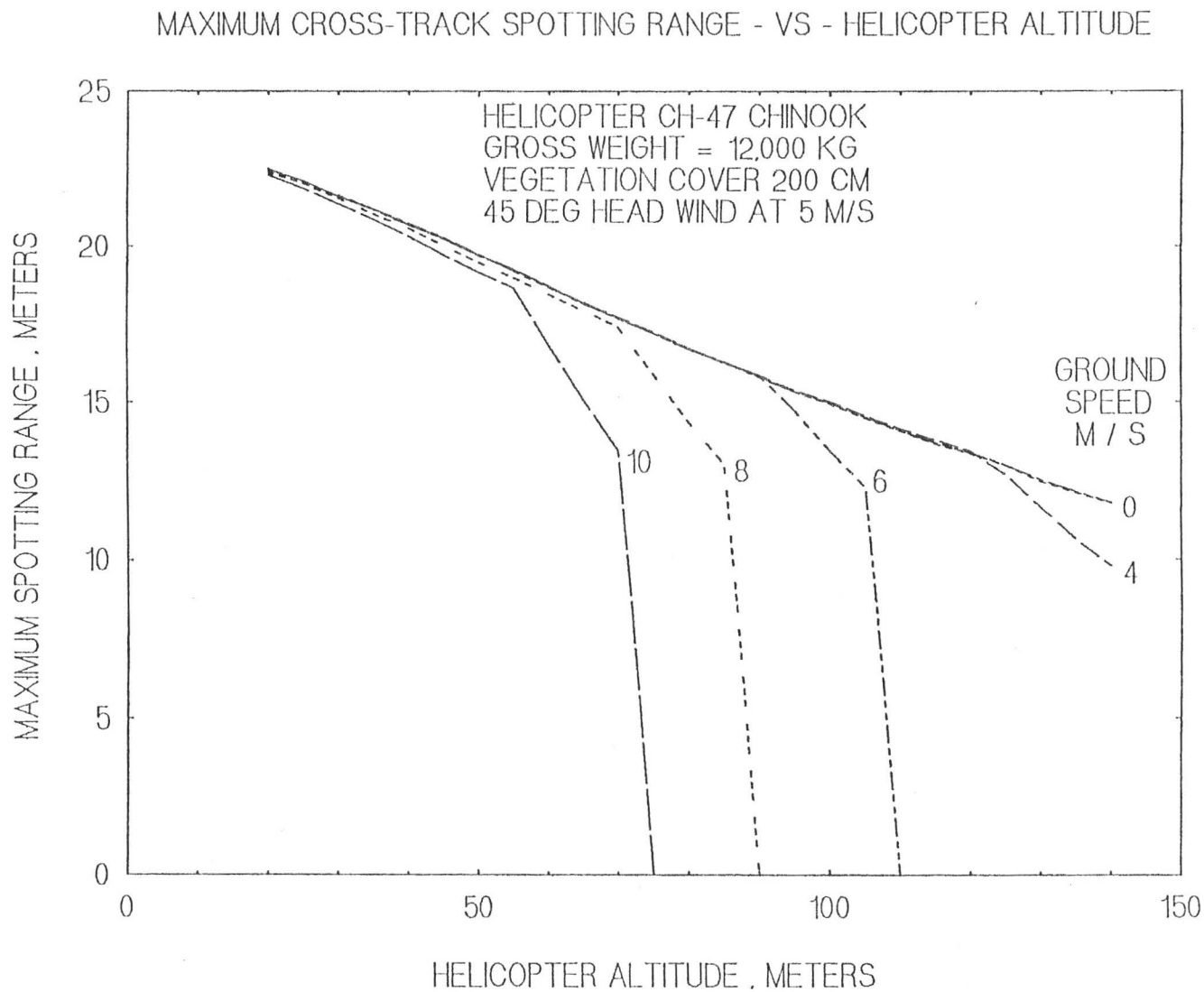

Figure 10. Predicted maximum cross-track spotting distance as a function of altitude and ground speed for a CH-47 Chinook helicopter in near minimum gross weight condition, flying into a head wind of 5 m / s at 45 degrees to its ground track over vegetatic a height of 200 cm. The breaks in the curves are discussed in the text.

4, 6, 8, and 10 are examined. The wind (considered to be constant with altitude) is blowing at 5 m / s at 45 degrees to the ground track, generally counter to the direction of travel of the helicopter.

Note the following features of the curves shown in this figure: First, below about 55 m altitude, the ground speed of the helicopter seems not to be important in establishing cross-track spotting distances. This is because the downwash flow field impinging on the surface is sufficiently strong to lift the smallest viable firebrands to initial flight conditions that keep them moving along with the outwash field as it moves along behind the helicopter. But as the altitude increases, the downwash flow field that impinges the surface becomes weaker until, at some point, the smallest viable firebrand particles can no longer be transported by the outwash flow fast enough in the direction of helicopter travel to keep up with the aircraft, without a penalty in the lateral transport distance attainable. The onset of this situation causes the first break in the distance - versus - altitude graphs. The second break in the "high speed" curves is due to the predicted demise of the flow field model due to the excessive bending of the downwash flow field under the influence of the relative air speed. The maximum spotting distance undoubtedly does not fall abruptly to zero under these specific conditions. It is simply the case that the model cannot be trusted to predict the distance with useful fidelity.

Figure 11 shows the maximum along-track spotting distances for conditions identical to figure 10. Note that the higher the helicopter true ground speed (at low altitudes) the greater the predicted along-track spotting distance. This is because the firebrand particle is being pushed along in front of the helicopter by the outwash field. But this situation changes abruptly when the downwash (and hence the outwash) flow weakens sufficiently because of the added entrainment that accrues when the downwash flow travels far

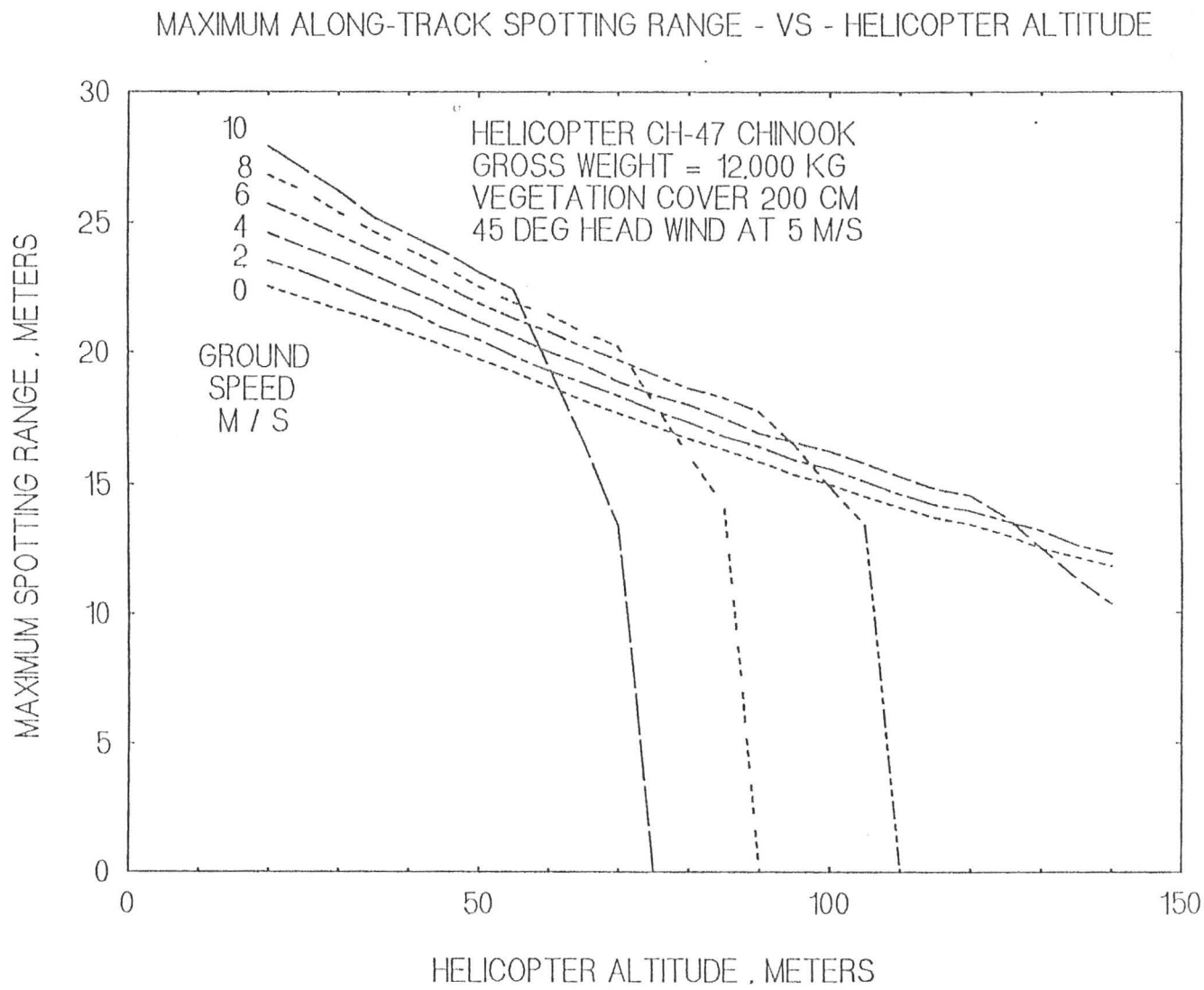

Figure 11. Predicted maximum along-track spotting distance for the conditions of figure 10.

enough through the ambient air before impinging upon the surface. The breaks in the curves of figure 11 occur at the same conditions as in figure 10, and for the same reasons.

Figure 12 shows the predicted maximum spotting distance calculated without regard to direction for the conditions of figures 10 and 11. In fact, this figure is simply the greater of the two corresponding curves in the previous two figures. Under the conditions of these figures, the greatest spotting distance is always along the ground track of the helicopter.

Figures 13 and 14 are counterparts to figures 10 and 11. The only condition that has changed is the depth of the vegetation cover layer, which has shrunk to 20 cm in figures 13 and 14. The effect is not significant, and this is not surprising, as it is only the last 180 cm of height drop in the particle trajectory that can extend the spotting range. These results suggest that vegetation cover height might well be a parameter that can be suppressed for expediency.

Figures 15 and 16 are also counterparts to figures 10 and 11. In figures 15 and 16, the wind direction has been changed to a 45 degree tail wind. The effect of this change should be to reduce entrainment into the downwash flow because the air speed of the helicopter is reduced. This should increase the velocity of the downwash flow as it impinges the surface, increasing the capability of the outwash flow to transport firebrand particles. Comparisons (of figure 15 to figure10 and of figure 16 to figure 11) show that the maximum spotting distances in both directions has increased, in some cases by a substantial amount.

Finally, figures 17 and 18 show the influence of helicopter gross weight on predicted maximum spotting distances. Figure 17 is the counterpart to figure 10 and figure 18 to figure 11. In the latter figures, the

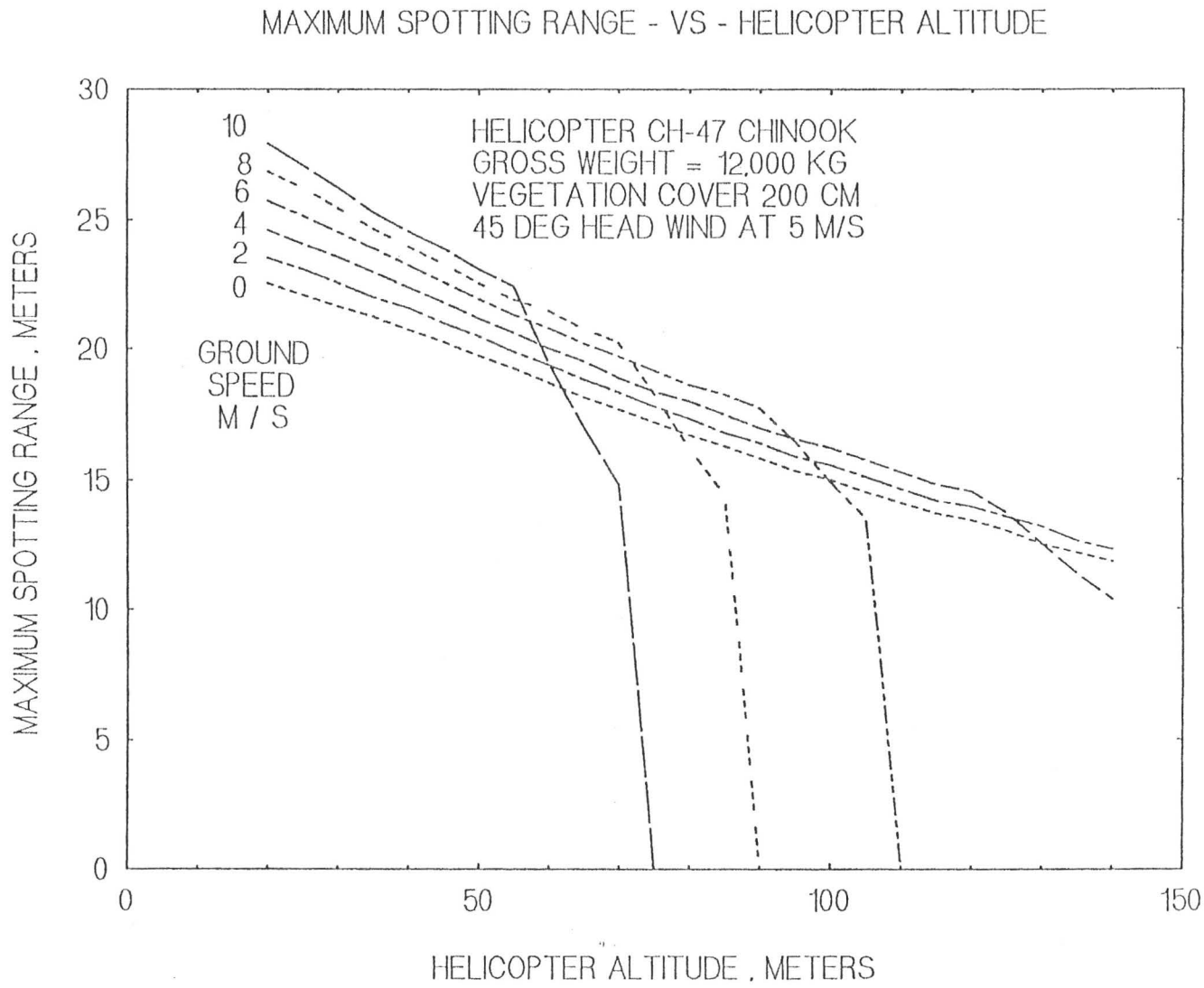

Figure 12. Predicted maximum spotting distance (regardless of direction) for the conditions of figure 10. Note that these curves are, at each point, the great the corresponding curves of figures 10 and 11.

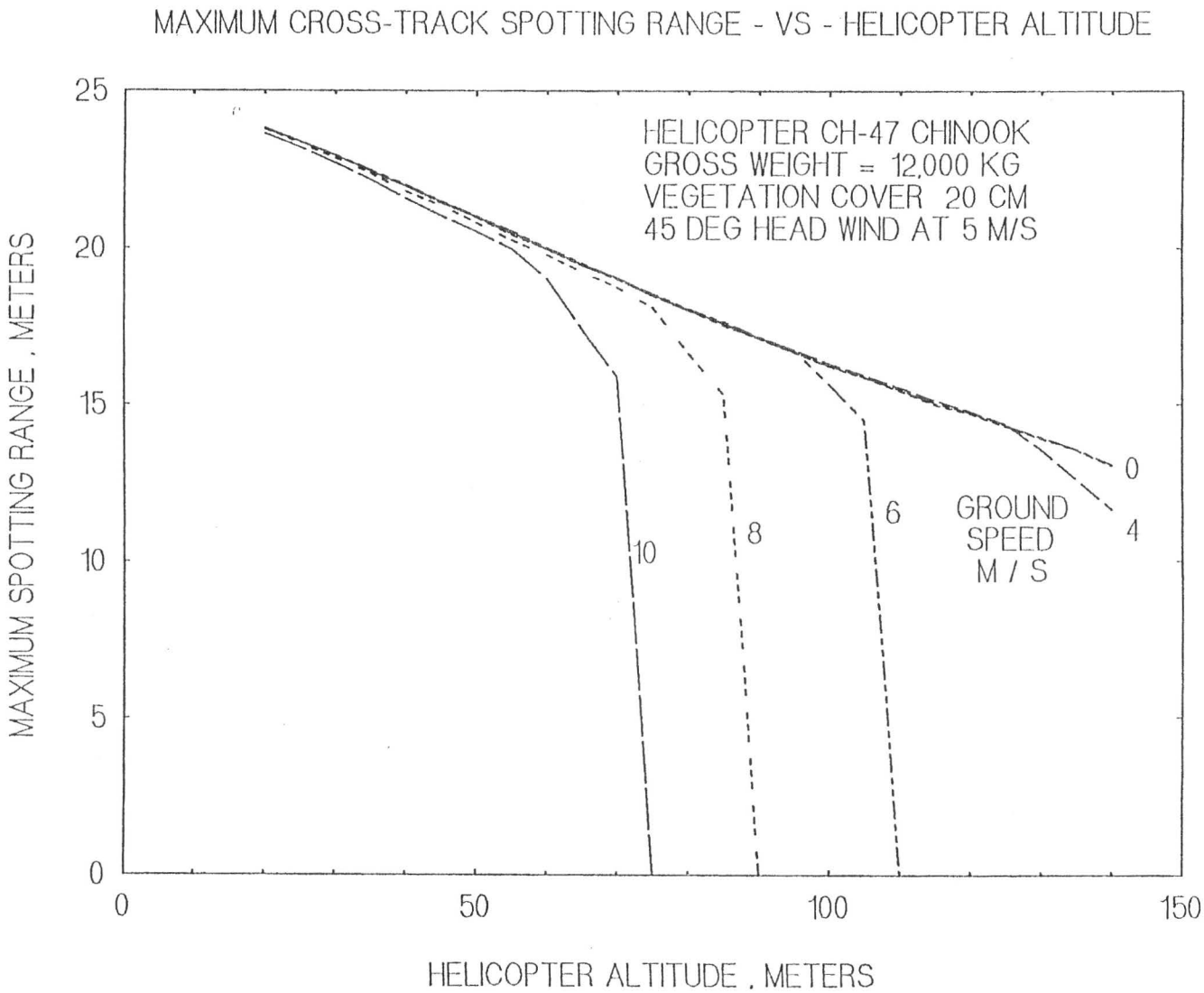

Figure 13. Predicted maximum cross-track spotting distance for the conditions of figure 10, except that the vegetation cover height is 20 cm instead of 200 cm. Note the increase in spotting distance compared to figure 10.

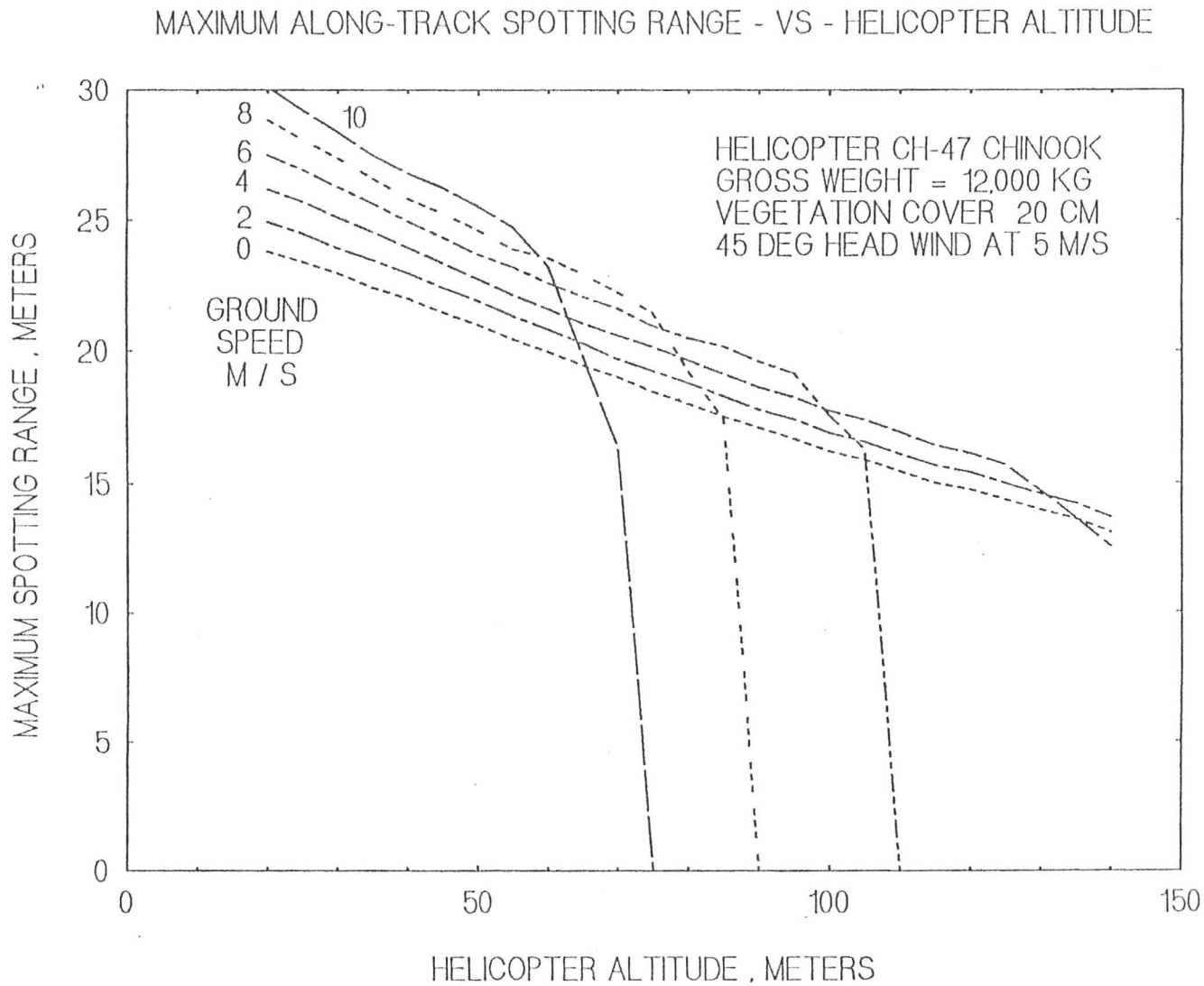

Figure 14. Predicted maximum along-track spotting distance for the conditions of figure 13. Compare to figure 11 to see the difference in spotting distance due to vegetation cover height.

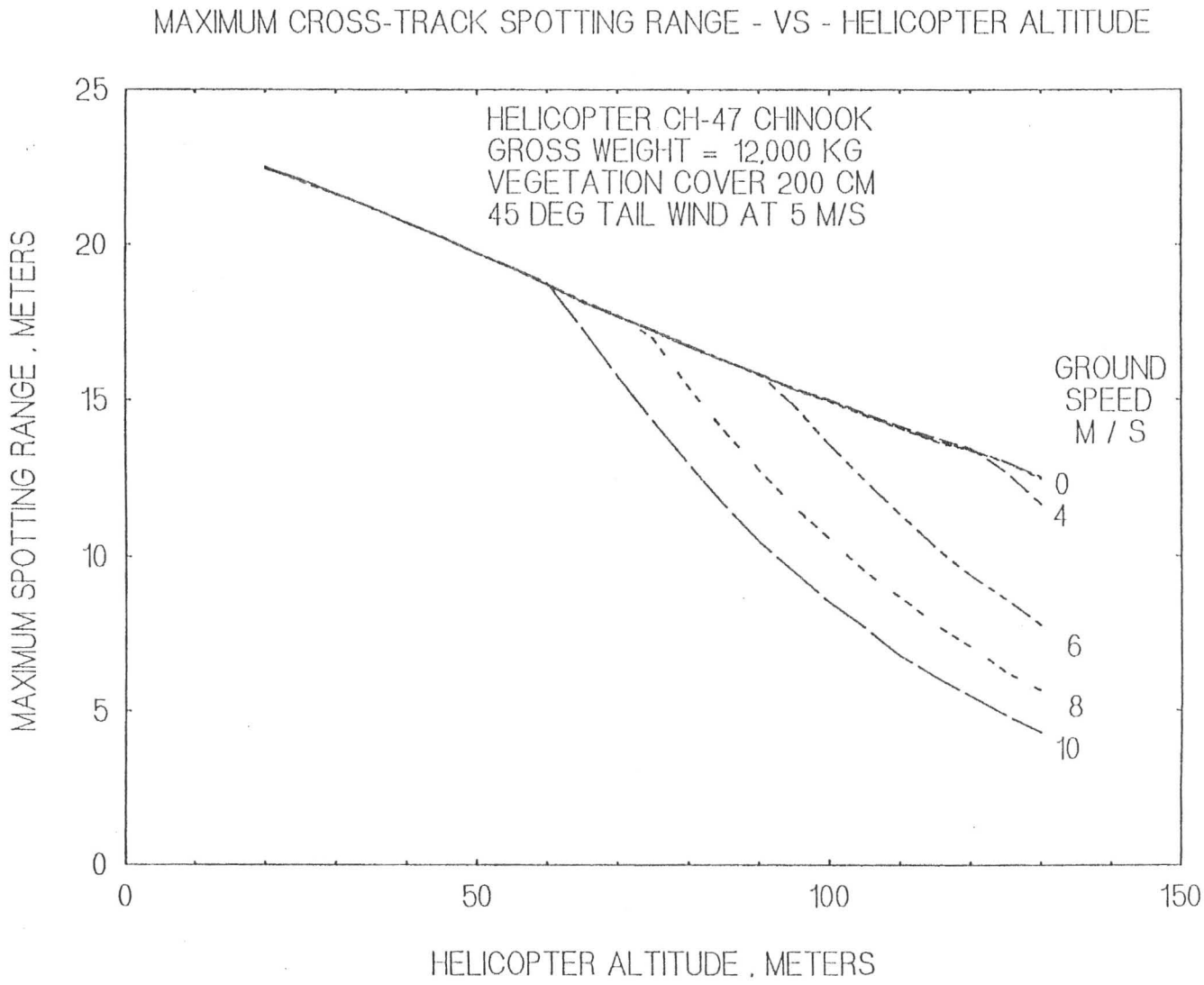

Figure 15. Predicted maximum cross-track spotting distance for the conditions of figure 10, except that the wind direction has been changed by 90 degrees to a 45 degree tail wind. Note that the breaks in the curves are less severe and that the complete demise of the flow field model is avoided in this case.

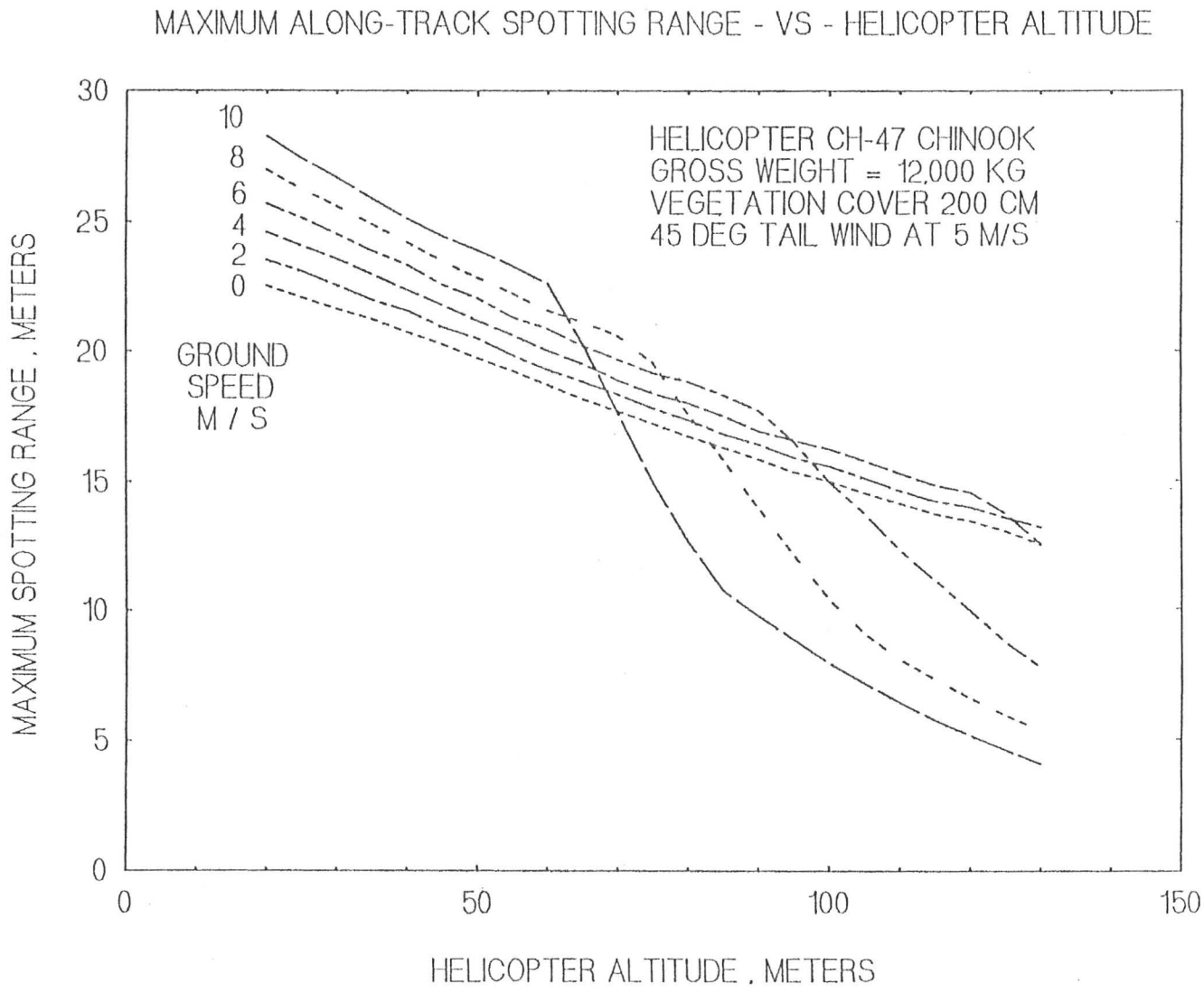

Figure 16. Predicted maximum along-track spotting distance for the conditions of figure 15. Compare to figure 11 to see the difference made by wind direction.

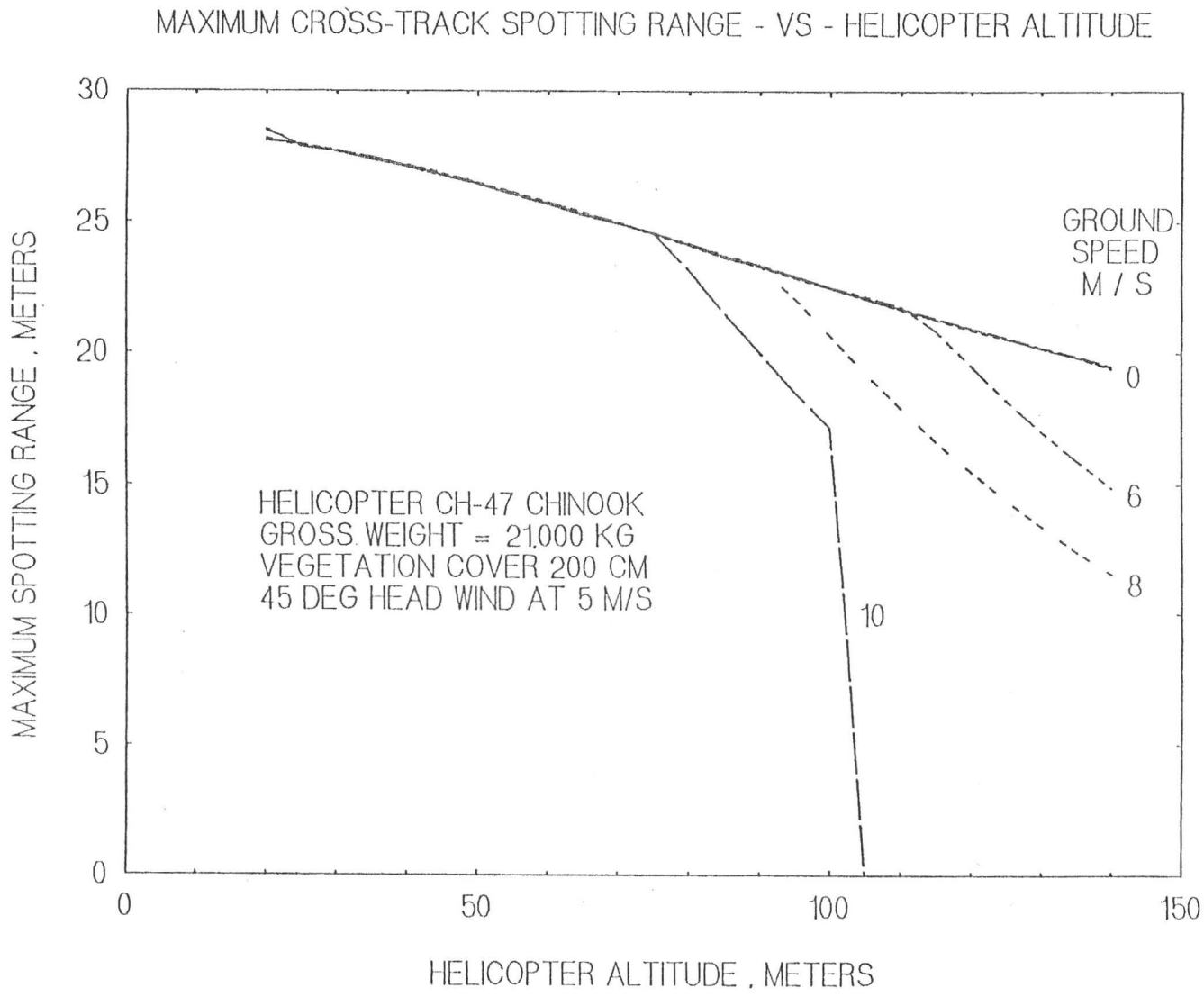

Figure 17. Predicted maximum cross-track spotting distance for the conditions of figure 10 except that the helicopter is nearly at its maximum gross weight. The higher downwash velocity required to support the heavier aircraft increases potential spotting distance.

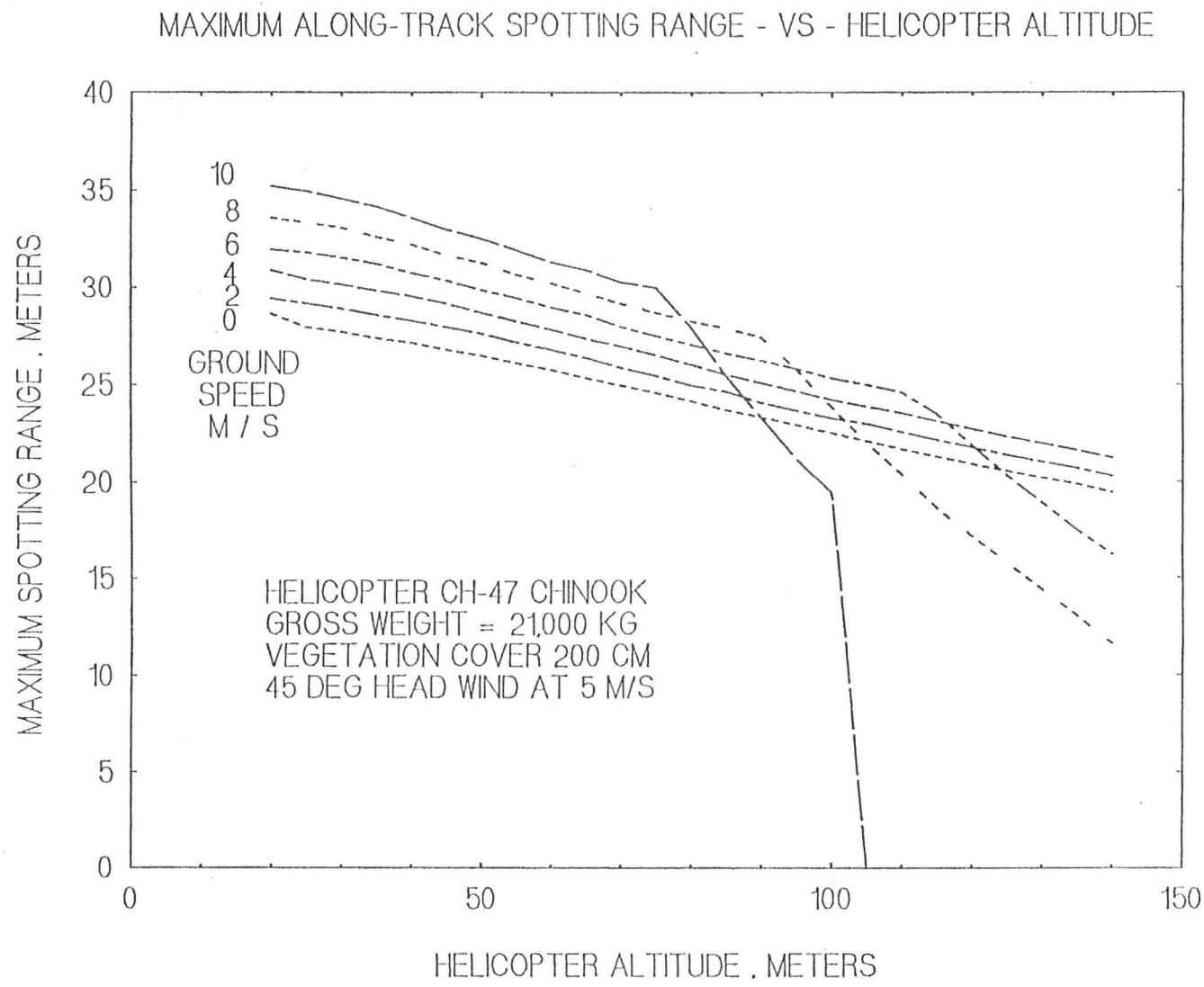

Figure 18. Predicted maximum along-track spotting distance for the conditions of figure 17. Compare to figure 11 to see the difference due to the greater eight of the helicopter in this case.

gross weight of the helicopter has been increased to 21 metric tonnes, near the maximum gross weight for the CH-47 helicopter. The increased downwash velocity required to maintain the heavier craft aloft has strengthened the outwash flow and postponed the demise of the model to much higher altitudes. The result is a significant increase in maximum spotting distance, both cross-track and along-track.

SUMMARY

A simplistic model for the flow field generated by a helicopter is established by treating the downwash created by the rotor(s) as a circular jet of incompressible fluid in a medium of the same properties. The model is rendered sensitive to movement of the ambient medium with respect to the axis of the downwash jet by the artifice of an arbitrary model that increases the rate of entrainment of ambient fluid by the jet as a function of the ratio of relative air speed to initial jet velocity. By taking account of the lateral momentum accretion of the jet, its direction of travel is predicted as a function of distance traveled. When the deflection angle of the downwash jet axis is predicted to reach 30 degrees from vertical at the place where the jet would reach the surface, the model is no longer to be trusted, in the viw of its author. The 30 degree figure is arbitrary, of course, and can easily be changed in the computer algorithms that implement model predictions.

The outwash flow field established when the downwash impinges on the surface is modeled in an elementary fashion that takes account of the accretion of ambient still air along the upper surface of the outwash flow field and of the equivalent shear stress exerted on its lower surface by the vegetation cover layer. The initial outward horizontal velocity is not sensitive to a vegetation cover layer's existence, so enhanced fire spread rate and/or flame length due to this wind created by the helicopter do not depend upon this parameter either. The model for the structure of the outwash flow field is sensitive to the

height of the vegetation cover, but only very slightly so, and example exercises of the firebrand transport prediction algorithms suggest that this sensitivity might well be suppressed for expediency.

Using these simplistic models an algorithm has been constructed for predicting the maximum distance over which a potential firebrand might be transported due to helicopter overflight of a fire. The algorithm accommodates and is sensitive to the following parameters: helicopter gross weight, effective rotor radius, flight altitude, and ground speed, wind speed and direction (relative to ground track), and vegetation cover height. The algorithm is embedded in an interactive FORTRAN program that runs under DOS on a PC. A listing of the computer source code and detailed instructions for use of the model are available from the USDA Forest Service, NWST, Missoula MT.

ACKNOWLEDGEMENT

The author gratefully acknowledges sponsorship of this research by USDA Forest Service NWST under Cooperative Research and Development Grant _____.

References

Albini, F. A., "Spot fire distance from burning trees – a predictive model", USDA Forest Service General Technical Report INT-56(1979) Available from USDA Forest Service Rocky Mountain Research Station, Ft. Collins, CO.

Albini, F. A., "A phenomenological model for wind speed and shear stress profiles in vegetation cover layers", Journal of Applied Meteorology **20**,11:1325-1335(1981a)

Albini, F. A., "Spot fire distance from isolated sources – extensions of a predictive model", USDA Forest Service Research Note INT-309 (1981b) Available from USDA Forest Service Rocky Mountain Research Station, Ft. Collins, CO.

Andrews, P. L., "BEHAVE: Fire behavior prediction and fuel modeling system – BURN subsystem, part I" USDA Forest Service General Technical Report INT-194 (1986) Available from USDA Forest Service Rocky Mountain Research Station, Ft. Collins, CO.

Andrews, P. L., and C. H. Chase, "BEHAVE: Fire behavior prediction and fuel modeling system – BURN subsystem, part II" USDA Forest Service General Technical Report INT-260 (1989). Available from USDA Forest Service Rocky Mountain Research Station, Ft. Collins, CO.

Briggs, G. A., "Plume rise" US Atomic Energy Commission, Division of Technical Information pamphlet TID-25075 (Nov. 1969).

Burgan, R. E., and R. C. Rothermel, "BEHAVE: Fire behavior prediction and fuel modeling system – FUEL subsystem" USDA Forest Service General Technical Report INT-167 (1984) Available from USDA Forest Service Rocky Mountain Research Station, Ft. Collins, CO.

Lee, S-L., and H. W. Emmons, "A study of natural convection above a line fire" Journal of Fluid Mechanics **11**,3:353-169(1961)

Marks, L. S., Ed., "Mechanical engineers handbook", fifth edition. McGraw-Hill, New York (1951). Table 5., p 255.

Press, W. H., S. A. Teukolsky, W. T. Vetterling, and B. P. Flannery, "Numerical recipes in FORTRAN; The art of scientific computing, second edition" Cambridge University Press, New York, [ISBN 0 521 43064 X] reprinted with corrections 1994. Chapter 16.6 *et seq*.

Ricou, F. P., and D. B. Spalding, "Measurements of entrainments by axisymmetrical turbulent jets", Journal of Fluid Mechanics **11**:21-32(1961).

Rothermel, R. C., "A mathematical model for predicting fire spread in wildland fuels" USDA Forest Service Research Paper INT-115(1972). Available from USDA Forest Service Rocky Mountain Research Station, Ft. Collins, CO.

Rouse, H., C. S. Yih, and H. W. Humphreys, "Gravitational convection from a boundary source", Tellus **4**:201-210(1952).

Taylor, G. I., "Dynamics of a mass of hot gas rising in the air" USAEC Report MDDC-919 (LADC-276), Los Alamos Scientific Laboratory, 1945. (Citation after Briggs, 1969).

Teske, M. E., and A. E. Kaufman, "Helicopter rotor wash effects on lateral fire spread", Technical Note No. 94-15, Continuum Dynamics Inc., Princeton NJ 08543, 1994. Also available from USDA Forest Service, 2121C Second Street, Suite 102, Davis CA 95616; Refer to contract 53-0343-4-00009, John Barry.

Teske, M. E., A. E. Kaufman, C. W. George, B. S. Grim, and J. W. Barry, "Field measurements of helicopter rotor was in hover and forward flight", American Helicopter Society Aeromechanics Specialist Conference, Fairfield County CT (1995).

Appendix A: Model for the downwash flow field

The downwash flow field is modeled as a uniform-velocity incompressible turbulent jet of circular cross section, directed vertically downward toward the surface. The jet entrains mass flow from the ambient air, with the entrainment coefficient modeled heuristically as a function of the crossing air speed, this being the resultant of the vector difference between helicopter velocity and ambient wind.

The jet arises from the action of the helicopter rotor blades, which accelerate the air downward and thus produce the upward thrust needed to support the weight of the helicopter. Of course, the flow initially does not have a uniform velocity. The velocity just below the rotor blades is greatest at the outer edge and least at the centerline. The flow must pass around the fuselage of the helicopter and reform into an organized structure beneath it. It is assumed that the flow merges into a stream of uniform velocity at this point and it is modeled as a jet below this confluence. The flow below the rotor plane is assumed to be in hydrostatic equilibrium.

The downwash jet is modeled analytically from its point of minimum cross sectional area just below the fuselage of the helicopter, where the jet radius is b_o and its downward velocity is represented by w_o. Let b and w stand, respectively, for the radius and velocity of the jet at distance z below the minimum area location, let v stand for the relative air speed acting normal to the jet, θ for the angle of the centerline of the flow, measured from vertical in the direction in which the wind tends to deflect the jet, and α the entrainment parameter [Taylor 1945]. Using these symbols and assumptions, the jet flow can be modeled by the following equations for the case when the flow is not significantly deflected from the vertical:

$$\text{(A1)} \qquad \frac{d}{dz}(\pi b^2 w) = \alpha 2\pi b w$$

$$\text{(A2)} \qquad \frac{d}{dz}(\pi b^2 w^2 \cos\theta) = 0$$

$$\text{(A3)} \qquad \frac{d}{dz}(\pi b^2 w^2 \sin\theta) = v\,\frac{d}{dz}(\pi b^2 w)$$

Equation (A1) expresses the rate at which mass flow is accreted into the downwash flow, the mean inflow velocity around the circumference of the jet being α times the downward velocity. Parameter α is called the entrainment parameter. The conservation of momentum flux in the vertical direction is expressed by equation (A2) and the rate at which the downwash flow accumulates horizontal momentum in the direction of the wind is expressed by equation (A3).

When v is small compared to w_o, the entrainment parameter can be taken to be α_j, the value for a turbulent jet into still air, which is 0.08 according to the classical measurements of Ricou and Spalding [1961]. But when v achieves a value comparable to or greater than w_o, entrainment would be replaced by simple incorporation of the impinging air stream on the upwind side, so (A1) would become:

$$\text{(A4)} \qquad \frac{d}{dz}(\pi b^2 w) = 2bv$$

Equating the right hand sides of equations (A1) and (A4) establishes that the value of α must change from α_j to $v/\pi w$ as v varies from zero to a value near w_o. To model this variation, an arbitrary function F(r) is introduced. This function varies from 0 to 1 in a sigmoidal fashion as its argument, $r = v/w_o$, varies from 0 to 1.

(A5) $$\alpha = \alpha_j + (r/\pi - \alpha_j) F(r); \qquad r = v / w_o$$

For F, the form below is used:

(A6) $$F(r) = r^2 (2 - r)^2$$

Because an upper bound is sought for the influence of rotor wash flow on fire behavior and potential spotting, deflection of the downwash flow by wind is neglected. It is assumed that the centerline of the flow field is vertical, but equations (A5) and (A6) are used to determine the value of the entrainment parameter. Using the approximation that $\theta = 0$, equations (A1-A3) yield immediately the variation of b and w with z, the distance downward from the helicopter altitude:

(A7) $$b = b_o + 2\alpha z ; \qquad w = w_o b_o / b$$

In order to establish a limiting value of z (*i.e.*, helicopter height) for a given value of v/w_o for which the approximation is valid that the flow is essentially vertical, an approximate solution for the deflection angl of the flow is obtained as follows. From equation (A2),

(A8) $$bw = b_o w_o / \sqrt{\cos\theta} ,$$

so equation (A3) becomes

(A9) $$b_o w_o \frac{d}{dz} \tan\theta = 2\alpha v / \sqrt{\cos\theta} .$$

Carrying out the differentiation gives the form

(A10) $$\frac{d\theta}{dz} = \frac{2\alpha v}{b_o w_o} \cos^{3/2}\theta .$$

For small values of θ the right hand side of equation (A10) is well approximated by

(A11) $$\frac{d\theta}{dz} \approx \frac{3\alpha v}{2 b_o w_o} \left(\frac{4}{3} - \theta^2 \right),$$

which can be integrated to give z as a function of θ:

(A12) $$\ln\left(\frac{\sqrt{4/3}+\theta}{\sqrt{4/3}-\theta}\right) = \frac{3^{3/2}\alpha}{2}\,\frac{v}{w_o}\,\frac{z}{b_o}\,.$$

The downwash flow field can not be well approximated as vertical if $\theta \approx 0.5$ or more, so a limit is established for the helicopter altitude, H_{max}, above which the flow field should deviate significantly from b and w in equations (A7), by using 0.5 for θ in equation (A12). Replacing b_o by the rotor radius b_h (see below) yields the limit:

(A13) $$\frac{H_{max}}{b_h} = \frac{1}{4\alpha\,\frac{v}{w_o}}\,.$$

This relationship, using equation (A5) with $\alpha_j = 0.08$, is plotted in figure 1. Since v is the magnitude of the air speed relative to the helicopter, it includes both helicopter and wind velocities.

To relate the minimum radius of the downwash flow, b_o, to the helicopter effective* rotor radius, b_h, it is assumed that the mass flow through the rotor plane is the same as that through the minimum area. The mass flow through the rotor plane is:

(A14) $$\dot{m} = \rho\,\pi\,b_h^2\,w_h$$

where w_h is air velocity downward into the top of the rotor plane, and ρ is the density of air. Assuming this to be the same as the mass flow through the minimum area,

(A15) $$\dot{m} = \rho\,\pi\,b_o^2\,w_o\,.$$

For static balance, the change in momentum flux must equal the gross weight of the helicopter, W_h, so:

(A16) $$W_h = \dot{m}\,(w_o - w_h) = \rho\,\pi\,b_h^2\,w_o^2\left\{\left(\frac{w_h}{w_o}\right)\left(1 - \frac{w_h}{w_o}\right)\right\}\,.$$

Now since the ratio w_h/w_o will be influenced by details such as rotor rpm and fuselage profile, the maximum value of 0.25 for the dimensionless factor in braces is used. This value is achieved when $w_h/w_o = 0.50$, which value was used to solve equation (A16) for w_o, as graphed in figure 2. It also provides the relationship between b_h and b_o used in equation (A13), namely that $b_o = b_h/\sqrt{2}$.

---

* If the helicopter has two rotors, an "effective rotor radius" is defined, this being the radius of a hypothetical single rotor that would have the same air flow area as do the two actual rotors combined.

Appendix B: Model for the outwash flow field

The jet-like downwash impinges on the surface, where it turns to flow radially outward in a thin, two-dimensional pattern. This flow is highly turbulent, especially in the central transition region where the mean flow is forced to turn from downward to outward. The radial outwash flow is impeded by friction at the surface and it accretes mass by entrainment. Both these effects tend to slow the mean radial velocity of the flow and thus to increase the thickness of the layer. The tendency to thicken is offset in part by the fact that the cross sectional area of the flow grows in proportion to the radial distance from the center of symmetry. Here a model is developed for the outwash flow field which includes the effects of friction due to vegetation cover and accretion of mass from quiescent ambient air. Boundary conditions at the inner edge of the outwash flow are imposed by conserving mass flow through the turning region and use of the assumption that half the kinetic energy of the impinging jet is lost in the transition to radially outward flow. Air is assumed to be incompressible and entire flow field treated as being in hydrostatic equilibrium.

Wind flow within and over vegetation cover layers has been modeled by the author [Albini 1981a]. In that model, the mean velocity of fully developed flow through the vegetation cover exhibits an essentially exponential profile with height, with velocity at the ground surface being about 20% of that at the upper edge of the vegetation layer. The flow through the vegetation layer is impeded by aerodynamic drag that is balanced by shear stress at the top surface, with a friction coefficient that tends to be constant at about 0.32. Using this mental picture of the outwash flow field allows the establishment of a crude model for the flow field that is sensitive to vegetation cover height and yet is analytically tractable.

Radial velocity u above the vegetation cover is treated as being constant at $u = u_c$. This is the "slug flow" idealization often used for highly turbulent situations. Within the vegetation (*i.e.*, $z' \leq h_c$) the velocity is assumed to decrease exponentially from u_c at $z' = h_c$ to $0.2u_c$ at $z' = 0$. This leads to the following expressions for mass and momentum fluxes at radius r :

$$\text{(B1)} \qquad \dot{m} = \text{radial mass flux} = 2\pi r\rho \int_0^h u(r,z')dz' \approx 2\pi r\rho u_c (h - 0.5 h_c)$$

$$\text{(B2)} \qquad \dot{f} = \text{radial momentum flux} = 2\pi r\rho \int_0^h u^2(r,z')dz' \approx 2\pi r\rho u_c^2 (h - 0.7 h_c)$$

where ρ is the density of air and h the depth of the outwash flow layer at radius r.

The rate of accretion of mass is modeled using an entrainment parameter α_w, which is expected to be approximately 0.16 based upon measurements of buoyant plumes from line sources [Rouse, Yih, and Humphreys 1952; Lee and Emmons 1961]. The entrainment flow is thought to be better approximated by that of a buoyant line plume than by a circular jet, with the entrainment parameter being about twice that for a jet. Introducing the friction coefficient C_f and the entrainment assumption gives the following flow field model:

(B3) $$\frac{d}{dr}\left\{ru_c\left(h - 0.5h_c\right)\right\} = \alpha_w r u_c$$

(B4) $$\frac{d}{dr}\left\{ru_c^2\left(h - 0.7h_c\right)\right\} = -\frac{1}{2}C_f r u_c^2$$

Finally, this model can be rendered analytically tractable by the approximation that $0.5h_c$ and $0.7h_c$ can both be replaced by $0.6h_c$:

(B5) $$h - 0.5h_c \approx h - 0.7h_c \approx h - 0.6h_c \equiv h^*$$

Introducing this approximation into equations (B3) and (B4) and expanding the left hand side of equation (B4) to make use of (B3) yields:

(B6) $$\alpha_w r u_c^2 + r u_c h^* \frac{du_c}{dr} = -\frac{1}{2}C_f r u_c^2$$

which can be rewritten as:

(B7) $$h^* \frac{d}{dr}\ln(u_c) = -(\alpha_w + \frac{C_f}{2}).$$

Dividing equation (B3) by ru_c, and expanding the left hand side yields:

(B8) $$\frac{dh^*}{dr} + \frac{h^*}{r} + h^* \frac{d}{dr}\ln(u_c) = \alpha_w \Rightarrow \frac{dh^*}{dr} + \frac{h^*}{r} = 2\alpha_w + \frac{1}{2}C_f.$$

This equation can be integrated to give h* in terms of an undetermined constant, A, and the result used in equation (B7) to find u_c, as follows:

(B9) $$h^* = \frac{A}{r} + (\alpha_w + \frac{C_f}{4})r$$

(B10) $$u_c (r h^*)^{\gamma} = \text{constant} = B, \text{ where } \gamma = \frac{2\alpha_w + C_f}{4\alpha_w + C_f}$$

To establish values for constants A and B, the mass flow within the impinging downwash jet is set equal to that in the outwash flow field where they meet. The streamlines dividing the downwash and outwash flow fields meet at radial distance r_s from the downwash jet centerline, at height $h_s = h^*(r_s) + 0.6h_c$, and thus a distance $H - h_s$ below the helicopter at height H. According to equation (A7) the radial coordinate r_s is related to this distance by:

(B11) $$r_s = b(z)\big|_{z = H - h_s} = b_o + 2\alpha(H - h_s)$$

and the vertical velocity w_s of the impinging downwash flow at this height is given by

(B12) $$w_s = w_o b_o / r_s .$$

Equating the mass flow downward through the circular area of radius r_s to that radially outward in the layer of height h_s at radius r_s provides the relationship:

(B13) $$\pi r_s^2 w_s = 2\pi r_s (h^*(r_s) + 0.6 h_c) u_s ,$$

where u_s is the value of u_c at radius r_s and $h^*(r_s)$ is the value of h^* at radius r_s.

Finally, to estimate the loss of kinetic energy of the air making the right angle turn at the surface, it is assumed that the loss is the same as that of water flowing through a smooth 90 degree elbow with the centerline radius equal to the diameter of the pipe. This gives a friction loss (loss due to induced local turbulence) of 50% of the incident kinetic energy [Marks 1951], so that u_s and w_s are related by:

(B14) $$u_s = w_s / \sqrt{2} .$$

Equations (B9) and (B10), with constants A and B evaluated using equations (B11) - (B14), were used to plot the figures in the text showing the bounding streamline of the complete flow field and the radial dependence of the outwash velocity. These equations also suffice to provide the maximum horizontal outwash velocity as a function of the parameters w_o, b_h, H, and α (or v, which, with w_o, determines α). The maximum horizontal flow speed in turn determines the maximum influence of outwash flow velocity on the rate of spread and flame length of the surface fire. The model for this influence is described in the text.

Appendix C: Spread rate and flame length dependence on wind speed

The BEHAVE fire behavior prediction system [Burgan and Rothermel 1984, Andrews 1986, Andrews and Chase 1989] employs the formulation of Rothermel [1972] to predict the influence of wind speed on fire spread rate. Rothermel's formulation relates wind driven fire spread rate, R, to the zero-wind spread rate, R_o, using a multiplying factor in the form:

$$R = (1 + \phi) R_o \qquad (C1)$$

The factor ϕ Rothermel related to the wind speed acting at midflame height, U by means of a power law correlation (for U less than a maximum value that depends on the fire's area intensity):

$$\phi = b U^a , \qquad (C2)$$

where a and b are empirically established constants that depend upon the fuel description.

The prediction of flame length in the BEHAVE system rests upon Byram's empirical formula [see, *e.g.* Rothermel 1972]:

$$L = K (R w H)^{0.46} \qquad (C3)$$

where L is the flame length, K is a constant that depends upon the system of units employed, and the product in parentheses (rate of spread, R, times fuel consumed per unit burned area, w, and specific heat of combustion of the fuel, H) is the fire line intensity (*e.g.*, kW / m or Btu / ft s). From this form it is easy to see that the flame length for a wind-aided fire, L, is related to the zero-wind flame length, L_o, by the equation

$$L = L_o (1 + \phi)^{0.46} \qquad (C4)$$

because L_o is given equation (C3) with $R = R_o$ and the other factors are all constants.

Thus, to predict the effect of helicopter-induced winds upon the rate of spread of a fire, and/or its flame length, one need only to know the empirical constants a and b of equation (C2). Of course the parameter a depends upon the units of measure employed. Here the SI system is used, so the wind speed, U, is measured in meters per second.

Parameters a and b are given in table C1 for the thirteen generic fuel models of the BEHAVE system, for U expressed in meters per second. Figures C1 - C4 show the fire spread rate ratios (R / R_o) as a function of wind speed for these fuel models, and figures C5 - C8 show the flame length ratios (L / L_o). Using the methods described in the text, once the maximum outwash velocity is established, these figures can be used to predict the spread rate and flame length consequences of that velocity.

Table C1. Constants a and b of equation (C2) for the 13 fuel models of the BEHAVE system

No.	Depth (m)	Best fits typical fuels described as:	a	b
1	0.305	Short grass, stubble, grass tundra	2.070	4.082
2	0.305	Open pine grassy understory, wiregrass	1.830	3.370
3	0.762	Tall grass, unharvested grain, sawgrass	1.311	8.764
4	1.830	Mature chaparral, manzanita, red slash	1.420	5.531
5	0.610	Young chaparral, laurel, vine maple	1.395	6.711
6	0.762	Low pocossins, dormant brush, shrub tundra	1.341	6.329
7	0.762	Palmetto-gallberry, southern rough	1.335	6.908
8	0.061	Compact closed timber litter	1.490	2.187
9	0.061	Fresh, uncompacted hardwood litter	1.719	2.460
10	0.305	Decadent conifer, shrub understory	1.431	3.092
11	0.305	Light conifer logging slash (< 100 T / Ha)	1.152	3.905
12	0.701	Clearcut conifer slash (100 - 300 T / Ha)	1.133	3.502
12	0.914	Heavy clearcut conifer slash (> 300 T / Ha)	1.140	3.086

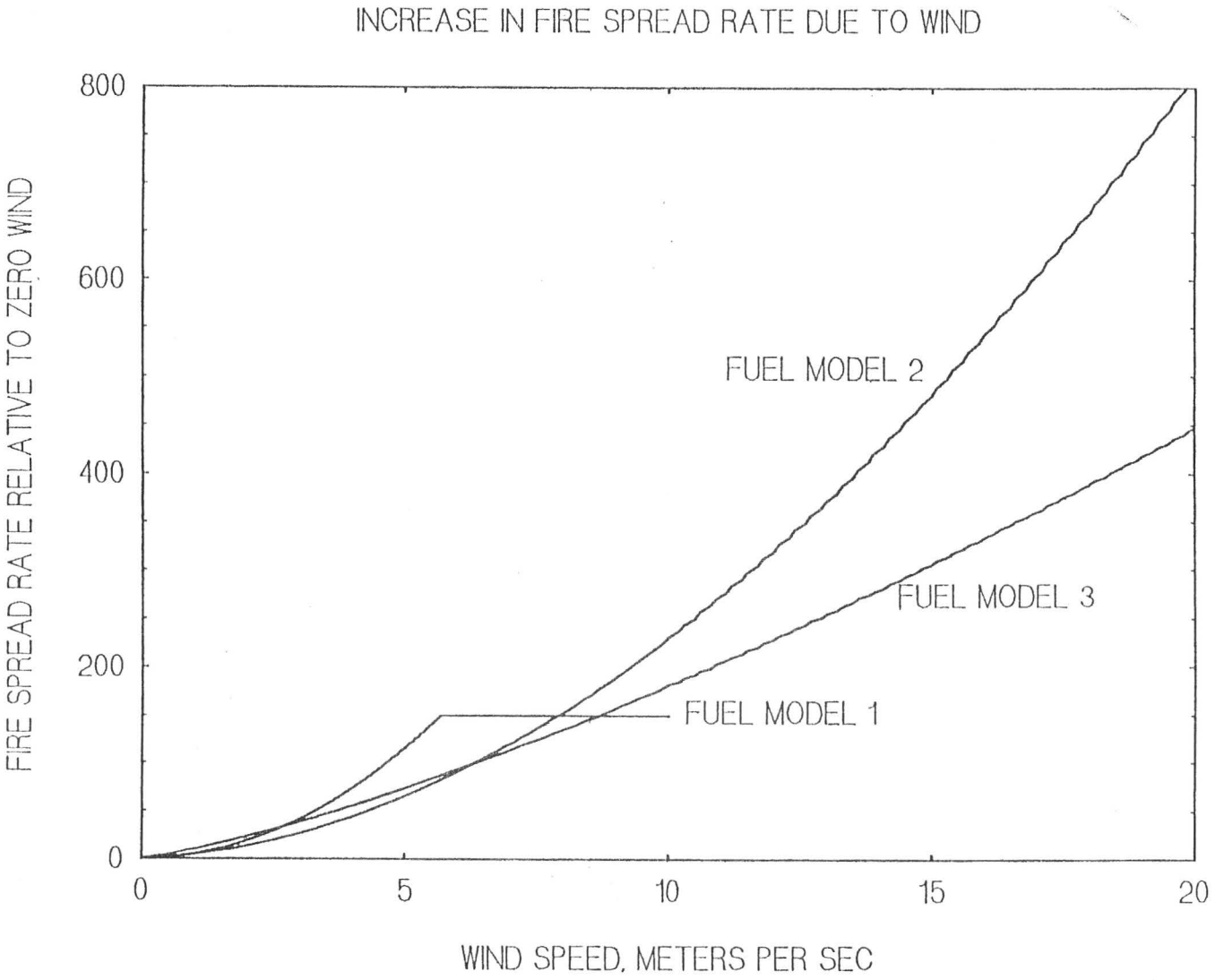

Figure C1. Fire spread rate multiplying factors for grass fuel models 1 -3.

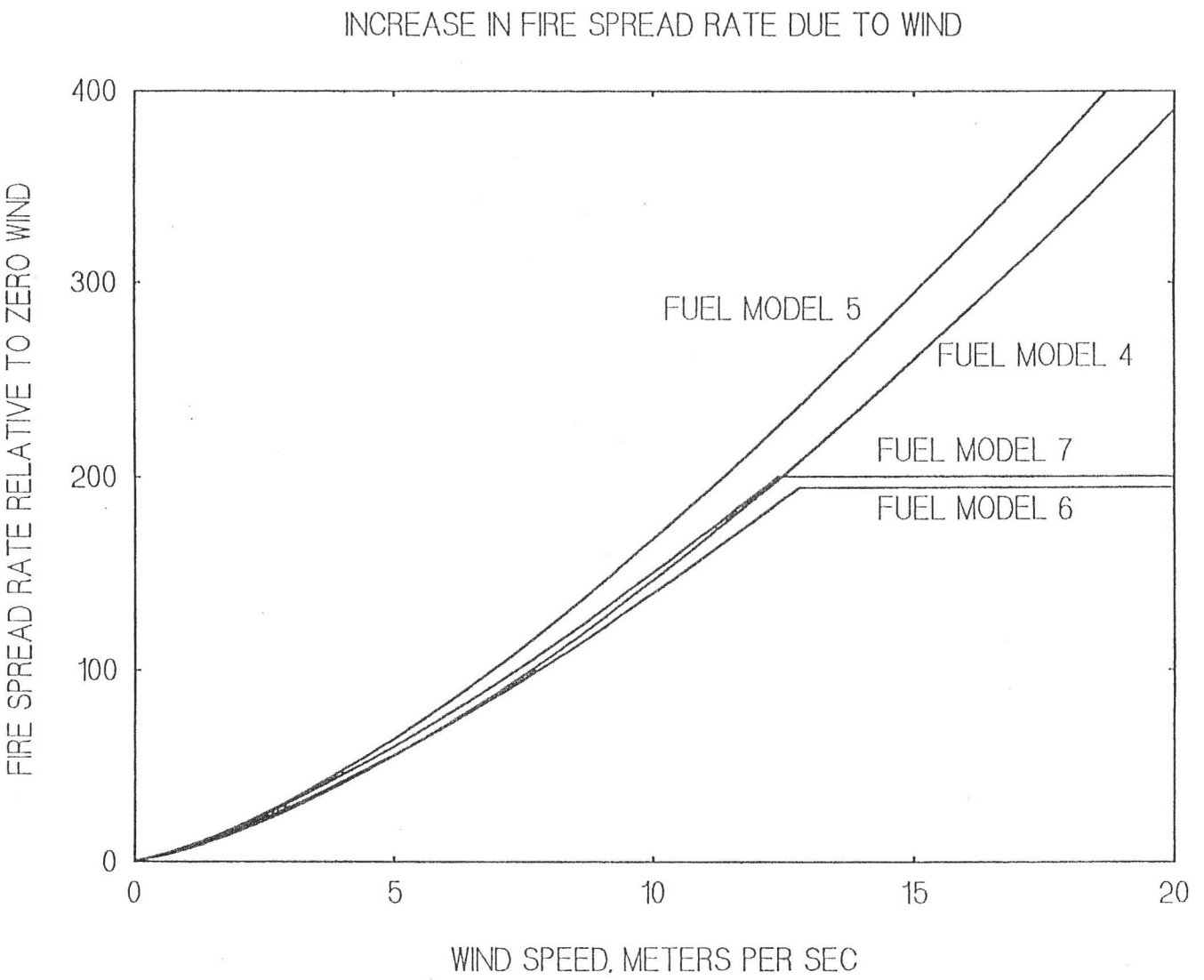

Figure C2. Fire spread rate multiplying factors for shrub fuel models 4 - 7.

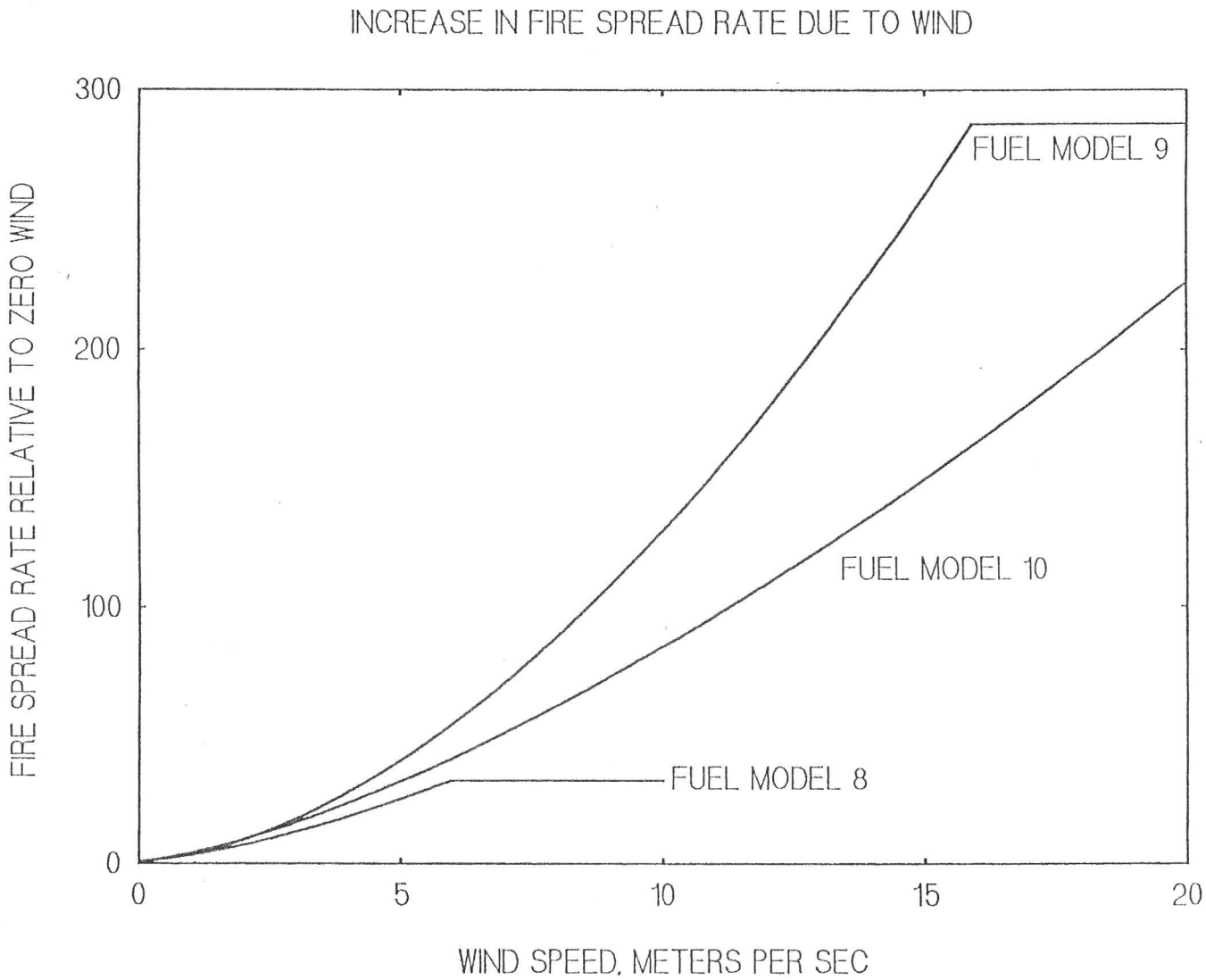

Figure C3. Fire spread rate multiplying factors for litter and understory fuel models 8 - 10.

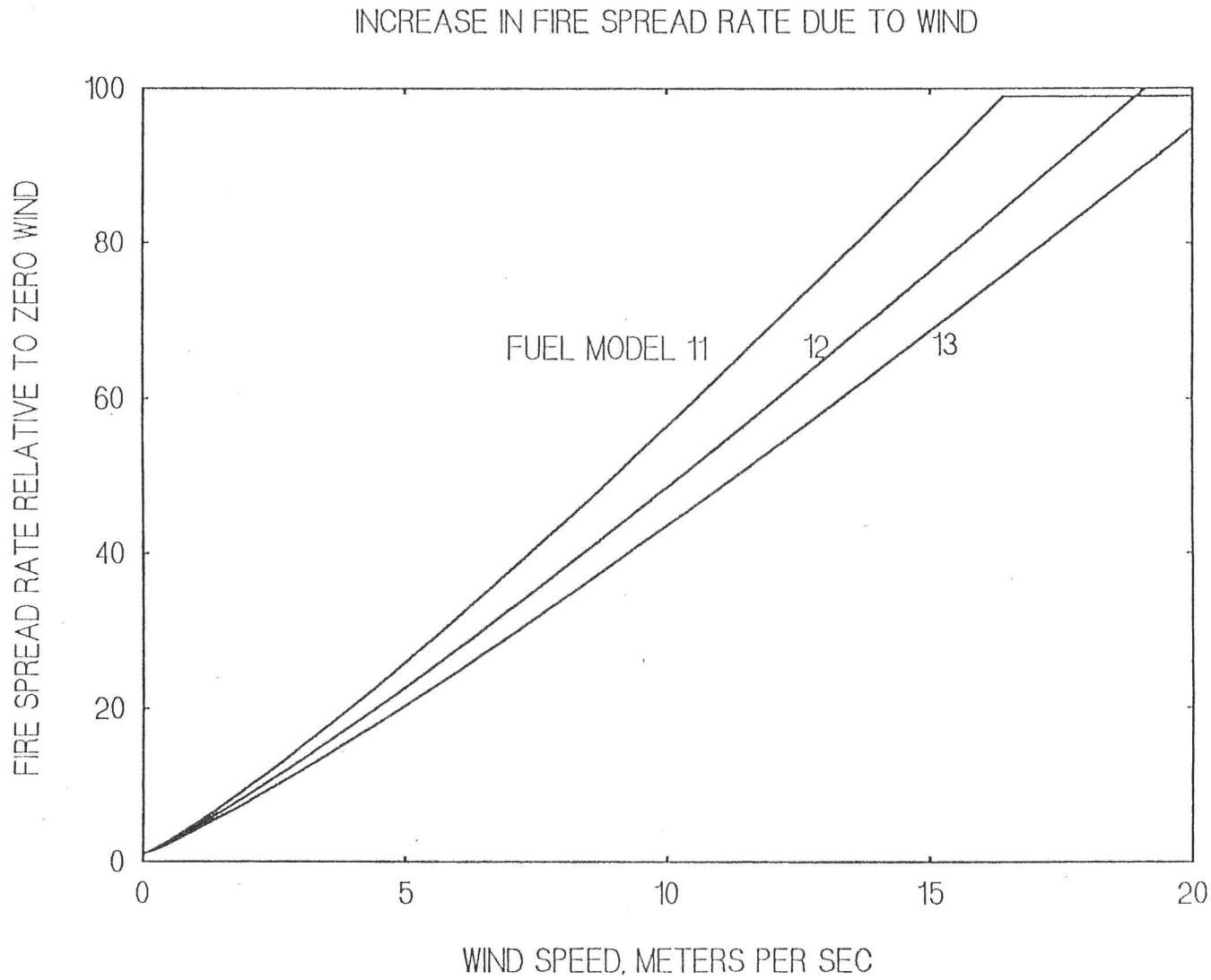

Figure C4. Fire spread rate multiplying factors for slash and harvest debris fuel models 11 - 13.

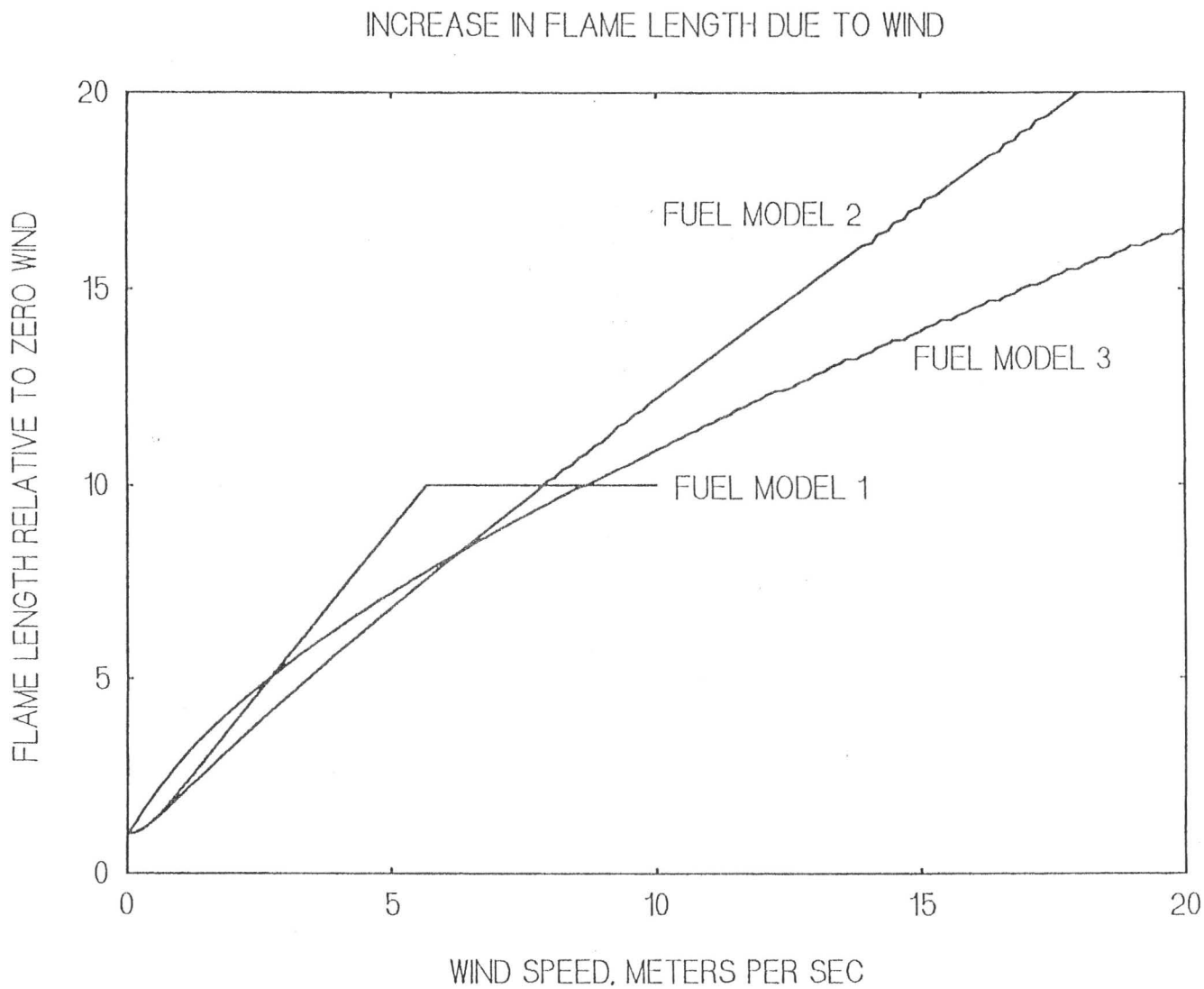

Figure C5. Flame length multiplying factors for grass fuel models 1 -3.

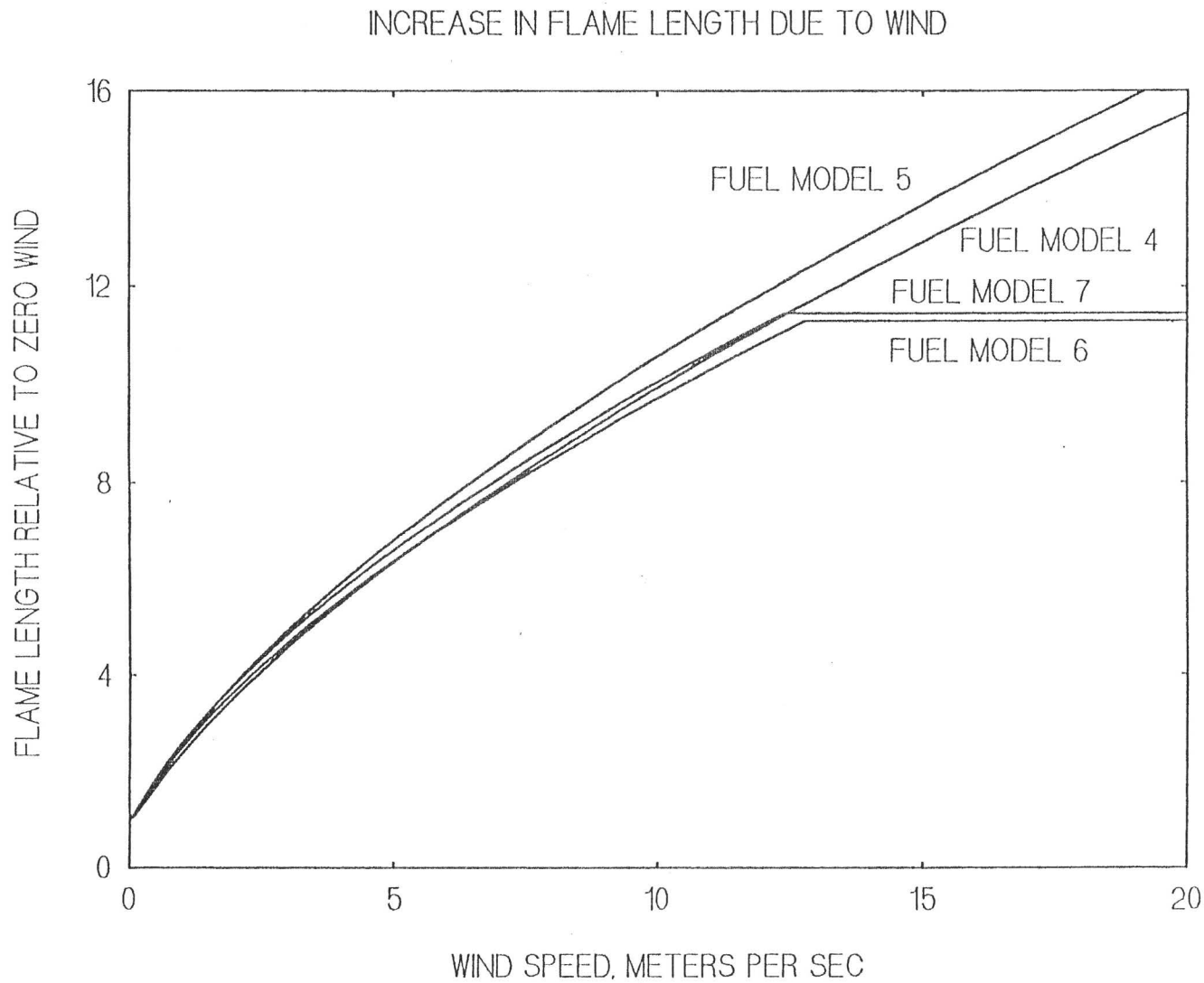

Figure C6. Flame length multiplying factors for shrub fuel models 4 - 7.

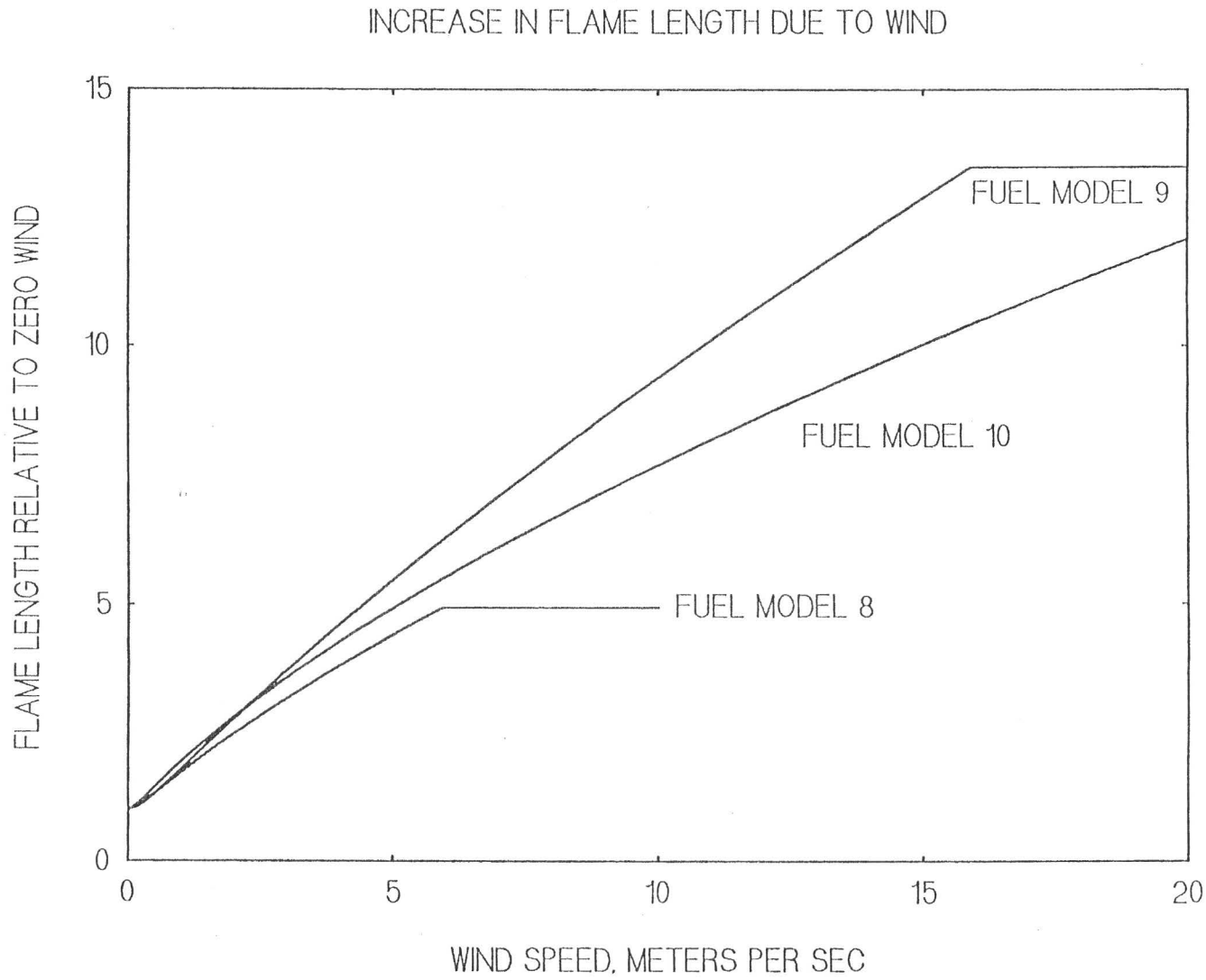

Figure C7. Flame length multiplying factors for litter and understory fuel models 8 - 10.

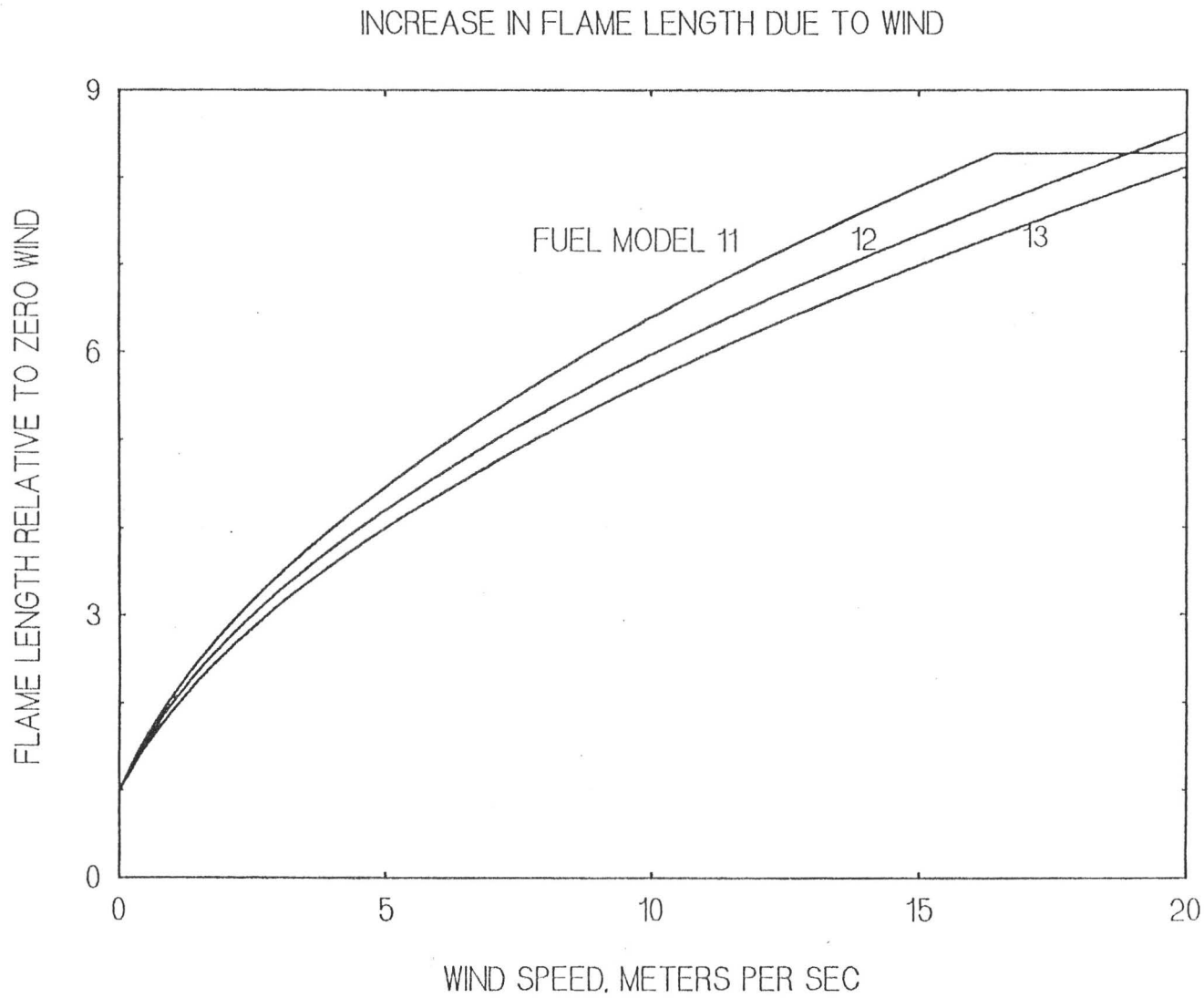

Figure C8. Flame length multiplying factors for slash and harvest debris fuel models 11 - 13.

Appendix D: Lift and transport of firebrands by rotor wash flow fields

A model is described which allows prediction of the maximum distance from the fire edge to which helicopter rotor wash can transport firebrands which may result in immediate spot fires. Firebrands that can promptly start spot fires must be aflame as they are transported, or they may be transported while smoldering but burst into flame upon alighting. In either case the firebrand must not be completely reduced to char, and must have sufficient sensible thermal energy to establish and maintain flaming combustion once it comes to rest. This means that the firebrand particle may be only partly pyrolyzed to char and must have sufficient mass to withstand cooling while in transit yet retain enough thermal energy to sustain flaming combustion at the end of its flight. Since the flight time of firebrands is quite brief in this situation, burning of the particle as it travels is not modeled, but an allowance is made for a small amount of mass reduction in establishing the minimum particle size to be considered.

Limbwood specimens from a variety of tree species were burned in the high speed wind tunnel at the USDA Forest Service Intermountain Fire Sciences Laboratory to relate burning rate to relative wind speed [Albini 1979]. It was noted during these trials that, in many cases, the specimen would burn by glowing combustion in the wind stream but would burst into flame upon being removed from the wind tunnel for weighing and measuring. Although the data were not recorded, the author recollects that in order for this phenomenon to occur, the specimen had to have a residual diameter of at least 5 - 6 mm and to be no more than about 50% char. These figures are used as a guide in establishing the range of firebrand particle "sizes" (see below) that are explored to determine the particle that can travel the greatest distance and start a spot fire upon alighting.

The firebrand transport process starts with the lifting of a burning fuel particle to a height determined by the product of the density and diameter of the particle, the speed of the air that lifts it, and the length of time the lifting flow field exists. The wind that lifts the fuel particle is assumed to be a transient flow structure arising at the outer edge of the transition region where the downwash flow field impinges on the surface. The lifting wind velocity is modeled as being vertical at speed w_s, lasting no longer than t_{min}, the minimum of the times h_s/w_s and b_o/v. The first of these times is meant to represent the duration of the transient velocity and the second the time scale for the existence of the flow field in the vicinity of the particle to be lifted (see appendix A). A right circular cylinder of diameter D, length L with fraction 1 - f being wood of density ρ_w and fraction f being char of density ρ_c has mass m, where:

$$(D1) \qquad m = \pi\left(\frac{D}{2}\right)^2 L\left((1 - f)\rho_w + f\rho_c\right)$$

The upward velocity of the particle, v_p, will evolve according to:

$$(D2) \qquad \frac{d}{dt}v_p = \frac{1}{2}\rho_a\left(w_s - v_p\right)^2 C_D LD/m - g = \frac{2C_D\rho_a\left(w_s - v_p\right)^2}{\pi D\rho_w\left(1 - f + f\frac{\rho_c}{\rho_w}\right)} - g$$

as air of density ρ_a blows normal to the centerline of the particle straight upward at speed w_s. This equation contains a characteristic dimension, λ, which determines the trajectory of the particle:

$$(D3) \qquad \frac{d}{dt}v_p = \frac{\left(w_s - v_p\right)^2}{\lambda} - g \quad ; \quad \lambda = \frac{\pi\rho_w\left(1 - f + f\frac{\rho_c}{\rho_w}\right)}{2C_D\rho_a} D$$

Using typical values ($\rho_w = 550$ kg/m^3, $\rho_c = 110$ kg/m^3, $\rho_a = 1.16$ kg/m^3, $C_D = 1.2$, $f = 0.5$) the size of λ measured in meters is found to equal about 0.4 times the particle diameter in mm. So if the particle must be, say, 5 mm to start a spot fire, the value of λ must be at least 2 m when the particle alights.

Since w_s is constant, equation (D3) can be integrated for the "slip velocity" $\omega = (w_s - v_p)$:

$$(D4) \qquad \lambda\frac{d}{dt}\omega = g\lambda - \omega^2 \quad \Rightarrow \quad \ln\left(\frac{\sqrt{g\lambda} + \omega}{\sqrt{g\lambda} - \omega}\right) = 2\sqrt{\frac{g}{\lambda}}\,t + \ln\left(\frac{\sqrt{g\lambda} + w_s}{\sqrt{g\lambda} - w_s}\right)$$

From this form one can identify $\sqrt{g\lambda} \equiv w_t$ as the terminal falling velocity of the particle and note that the parameter group

$$(D5) \qquad \tau = \frac{1}{2}\sqrt{\frac{\lambda}{g}}$$

represents the aerodynamic response time of the particle. Equation (D4) can be manipulated to provide the particle's vertical velocity as a function of time which can then be integrated to provide the height of the particle as a function of time:

$$(D6) \qquad v_p = \frac{dz'}{dt} = \left(w_s - w_t\right)\left\{\frac{1 - e^{-\frac{t}{\tau}}}{\Omega - e^{-\frac{t}{\tau}}}\right\} \quad \text{where } \Omega \equiv \frac{w_s + w_t}{w_s - w_t}$$

which leads to the height - vs - time relationship

$$(D7) \qquad z' = \left(w_s - w_t\right)t + \lambda \ln\left\{\frac{1 - e^{-\frac{t}{\tau}}}{\Omega - e^{-\frac{t}{\tau}}}\right\}$$

To establish the initial conditions of the trajectory of a particle with characteristic dimension λ, equation (D7) is solved for the time required for the particle to reach height h_s, the initial height of the top of the

outwash flow layer. If the time required, t^*, is less than t_{min}, then the particle is assumed to have reached height h_s, and radius $1.10r_s$ in time t^*, and its speed is calculated from equation (D6) at that time. If t^* is greater than t_{min} then equations (D7) and (D8) are used to evaluate the height and speed of the particle at time $t^* = t_{min}$ and these values are used for initial conditions.

With the particle's initial height and speed established, it is placed at azimuth angle ϕ and radial distance $1.10r_s$ from the centerline of the downwash flow. The initial azimuth angle of its direction of travel, ϕ', is allowed to range from zero to the minimum of $(\phi + \pi/2)$ and π. The elevation angle of its initial velocity, ε, is allowed to range from 0 (horizontal) to $0.3\ \pi$ upward. From each initial position and velocity, the particle's trajectory is integrated numerically in Cartesian coordinates (x',y',z'). In this coordinate system, y' is measured horizontally along the direction $\phi = 0$, the direction of travel of the helicopter (and, with it, the flow field), z' is measured upward from the surface, and x' is horizontal and normal to the direction $\phi = 0$.

The path of the particle is followed until it falls into the vegetation cover, *i.e.*, until $z' = h_c$. At this time the value of its x' coordinate is reduced by the amount $1.10r_s\sin(\phi)$, its initial position along the x' axis, which is presumed to be at the fire edge. This reduced value of x' is identified as the potential lateral (cross-track) spotting distance for a particle of characteristic dimension λ launched from radial position $1.10r_s$, azimuth angle ϕ, with velocity determined as above, in a direction specified by azimuth ϕ' and elevation angle ε. Similarly, the y' coordinate where the particle alights is reduced by $1.10r_s\cos(\phi)$, its initial position along the y' axis. The azimuth angle for particle initial position (ϕ) is allowed to range from 0 to π and the characteristic dimension λ is varied from λ_{min} to $\lambda_{min} + 2.0$ in steps of 0.10 m. From this sweep through the parameter range the maximum spot fire distance in each direction is identified. In addition to the cross-track and along-track spotting distances, the total map distance that the particle travels from being lifted until it falls into the vegetation layer is computed and filed as well.

The minimum value of the parameter λ is calculated as $(2.0 + 0.01\ h_s)$ to allow for the reduction of λ to be expected as the particle falls from height h_s to the surface. According to the firebrand burning rate law [Albini 1979], the parameter λ decreases with time at a rate proportional to the relative velocity of the wind over the particle. If the particle moves horizontally at essentially the local air velocity, the relative velocity is equal to the falling speed, making λ decrease linearly with the particle's drop in height. The constant of proportionality between change in λ and change in height is about 0.01. Thus the particle should reenter the vegetation layer with the nominal value of $\lambda = 2.0$ needed to ignite a spot fire immediately, if it begins its descent with $\lambda = 2.0 + 0.01\ h_s$.

In the coordinate system used, lateral ("cross-track") spotting distance is measured perpendicular to the ground track of the helicopter, and longitudinal ("along-track") spotting distance is measured along the helicopter's ground track.